STRUCTURAL CORRELATIONS IN PENTACOORDINATE ZINC AND NICKEL SYSTEMS

A thesis submitted to the

UNIVERSITY OF CAPE TOWN

in fulfilment of the requirement for the degree of

MASTER OF SCIENCE

by

Thomas Paul Edwin Auf der Heyde B.Sc. (Hons) (Cape Town)

Department of Physical Chemistry
University of Cape Town
Rondebosch
7700
South Africa

March 1984

Thy crown and sceptre I will seize and regulate all my members
In stern severity, and cast thee out into the infinite
Where nothing lives, there to wander; and if thou returnest weary,
Weeping at the threshold of existence, I will steel my heart
Against thee to eternity, and never receive thee more.
Thy self-destroying, beast form'd Science shall be thy eternal lot.

WILLIAM BLAKE

INDEX

CONTENTS (i)

ACKNOWLEDGMENTS (ii)

PUBLICATIONS RESULTING FROM THIS WORK (iii)

ABSTRACT (iv)

INTRODUCTION 1

1. THE STRUCTURE CORRELATION PRINCIPLE
2. APPLICATIONS OF THE PRINCIPLE
3. THE AIM AND SCOPE OF THIS STUDY

DATA SEARCH AND STRUCTURE ANALYSIS 17

CORRELATIONS AND REACTION PATHWAYS 30

1. SUBSTITUTION REACTIONS AT ZINC
   (i) Berry Pseudorotation
   (ii) Substitution
2. SUBSTITUTION REACTIONS AT NICKEL
   (i) Association
   (ii) Pseudorotation
   (iii) Dissociation

DISCUSSION AND EXPERIMENTAL OBSERVATIONS 61

A CONCLUDING REMARK 68

APPENDIX 70

REFERENCES 78

ACKNOWLEDGMENTS

I wish to thank

Prof. Nassimbeni for all the help he has so willingly given me, both within the pages of this thesis and outside of them,

Karin for typing this manuscript so efficiently and helping me through its ups and downs,

the staff of the Computer Centre, University of the Western Cape,

the Universities of Cape Town and of the Western Cape, and the Council for Scientific and Industrial Research for financial assistance,

and

my parents for having had the depth to encourage me in everything I have chosen to do.

PUBLICATIONS RESULTING FROM THIS WORK

Reaction Pathways from Structural Data: Dynamic Stereochemistry of Zinc(II) Compounds. (*Acta Cryst.* - in press)

Reaction Pathways from Structural Data: Dynamic Stereochemistry of Nickel Compounds. (*Inorg. Chem.* - to be submitted)

ABSTRACT

The structure correlation principle has been applied to five-coordinate zinc and nickel complexes in order to map the mechanism for a bimolecular ligand substitution reaction at typical tetrahedral and square-planar centres. Evidence for the following mechanistic pathways is presented:

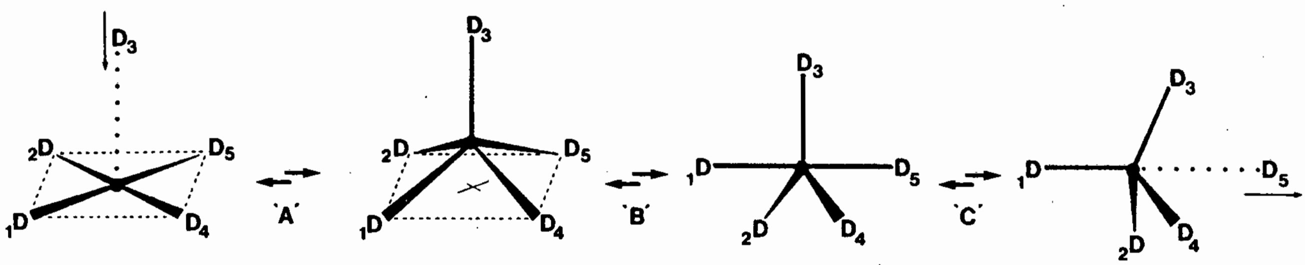

Tetrahedral zinc complexes are shown to undergo a reversible ligand association reaction (`C´), yielding a trigonal bipyramidal (TBP) intermediate, which can then either dissociate (`C´) or pseudorotate via the Berry mechanism (`B´) into a square-pyramidal (SQP) conformation. This latter step is shown to lead into a "cul-de-sac" in terms of dissociation of the intermediate, since TBP conformation seems to be a prerequisite for axial departure of the leaving group. Square planar nickel complexes are shown to undergo a reversible ligand association reaction (`A´) leading to a SQP intermediate, which may pseudorotate via the Berry mechanism (`B´) into a TBP. Dissociation of the five-coordinate intermediate may proceed either via apical departure from the SQP (`A´), or via axial departure from the TBP (`C´). The reaction coordinates thus derived are compared with theoretically predicted ones, and are supported by a large amount of experimental observations.

INTRODUCTION

THE STRUCTURE CORRELATION PRINCIPLE

The study of reaction mechanisms has traditionally involved the measurement of reaction rates, and the influence of temperature, concentration, solvent, and subtle molecular variations of the substrates on these rates. Although the results of such studies may yield some insight into the overall mechanism, they fail to define the detailed geometric changes which occur along the reaction pathway. In general the static molecular configuration of stable product and educt molecules, and in some cases that of stable intermediates, may be elucidated using tools such as X-ray crystallography. However, the dynamic aspects of such systems, dealing with the relative motion of the atoms during molecular distortions and transformations, ie., chemical reactions are not as easily uncovered. Information regarding the atomic motions (molecular deformations) occurring during a reaction, may, in some cases, be gleaned from the concept of an energy hypersurface characteristic of that particular reaction.

The Born-Oppenheimer approximation to the Schrödinger equations assumes the separation of nuclear and electronic motion, whereby the potential energy of a polyatomic system is calculated for a particular, static arrangement of the atomic nuclei. This calculation is then repeated for a range of other stationary arrangements, with the result that the energy hypersurface is represented as a scalar field in the Euclidian vector space spanned by the coordinates of the nuclei[1-5]. Stable arrangements of atoms, ie., stable molecules (products, educts or intermediates), correspond to minima, and will tend to aggregate in "dips" on the hypersurface. Curves connecting such minima along energy "valleys" and "passes" will represent minimum energy paths or reaction pathways (reaction coordinates). It is these curves which detail the synchronous changes in bond distances and angles as educt molecules are transformed to product molecules.

Pancir[1] has calculated the potential energy surface for the Diels-Alder reaction between ethylene and butadiene

$$C_2H_4 + C_4H_6 \rightleftarrows C_6H_{10}$$

as a function of four reaction angles ψ centred on the atoms between which bond formation occurs. His approach was based on a topological molecular orbital method[2] and involved the calculation of the Hartree-Fock energy. Figure 1a gives a three dimensional representation of a portion of the energy hypersurface, while Figure 1b shows the contour diagram which is obtained when the former is collapsed along the energy dimension onto the plane defined by the reaction angle parameters.

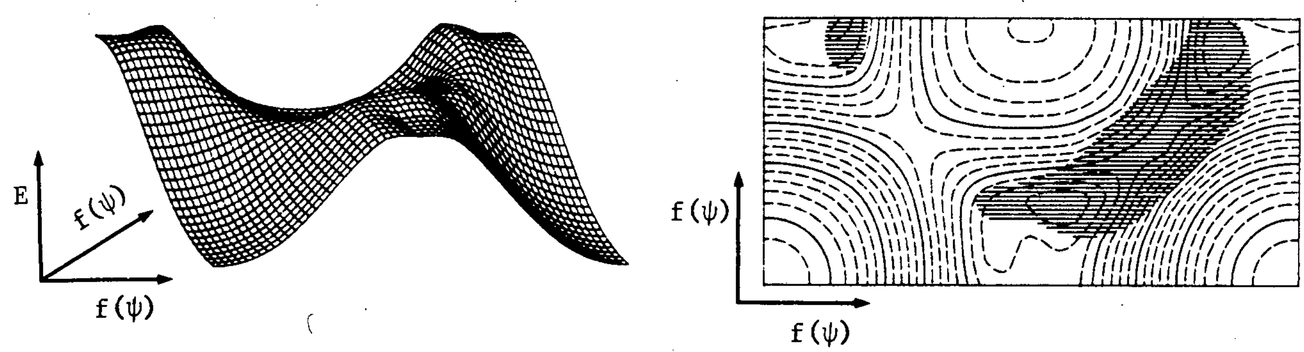

Figure 1. a) Three dimensional representation of the potential energy hypersurface for the Diels-Alder reaction. b) Contour diagram obtained when fig.1a is collapsed along the energy dimension. Contour lines indicate successive energy intervals. From ref.1.

Liu[3] has calculated *ab initio* the potential energy surface for the linear H_3 system, corresponding to the exchange reaction

$$H + H_2 \rightleftharpoons H_2 + H \qquad (1)$$

where the three hydrogen nuclei are assumed to lie in a straight line. This system is fully described by two parameters, these being the distances d_1 and d_2

$$\underset{d_1}{H\text{--------}}H\underset{d_2}{\text{——}}H$$

A contour diagram of the energy surface as a function of these parameters is shown in Figure 2, in which the two "dips" corresponding to the stable arrangement of a hydrogen atom and a hydrogen molecule, are connected via the minimum energy path shown as a broken line. It is this reaction coordinate which correlates the changes in d_1 and d_2 as the system progresses from the energy "well" at the top of Figure 2 to that on the right, ie., as the exchange reaction proceeds. Were it possible to isolate a number of stable, linear tri-hydrogen systems, for example in crystal structures, then it seems plausible to suggest that their representative points in the corresponding parameter space might well lie close to, or along, the reaction coordinate, which is, of course, an energy "valley", or a series of low lying points, in that space. Unfortunately no crystallographic investigations of linear H_3 systems have yet been reported, and it is therefore necessary to focus attention on other systems in support of the above hypothesis.

It is quite feasible that the linear exchange reaction

$$I^- + I_2 \rightleftharpoons [I_3]^- \rightleftharpoons I_2 + I^- \qquad (2)$$

will be characterised by a potential energy hypersurface similar to that calculated by Liu for reaction 1, and hence exhibit a similar hyperboloid relationship between the corresponding parameters. Bent[4] has graphically correlated the two distances describing an almost linear I_3^- fragment (bond angles 175° - 180°) found in a variety of different crystalline frameworks, and has obtained the hyperboloid relationship depicted in Figure 3a.

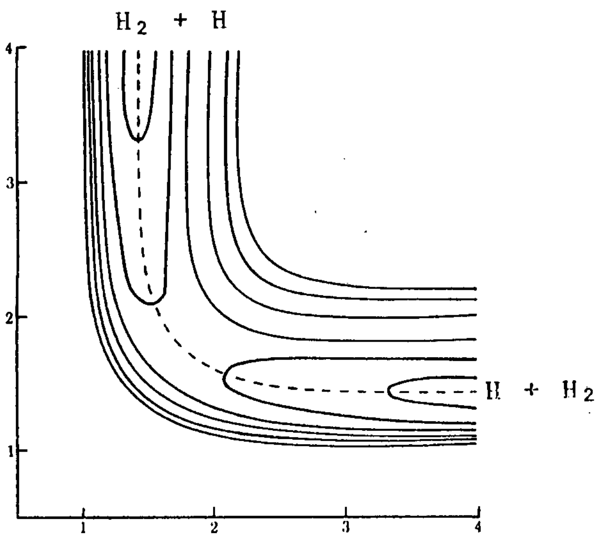

Figure 2. Potential energy surface for linear H_3 system. Distances are in Bohr units and contour lines are drawn at energy intervals of 0,01 hartrees. From ref.5a.

It seems as if the correlation found between the interatomic distance parameters describing the structure of the given I_3^- fragment in the various environments, maps a minimum energy pathway in the corresponding parameter space. This observation has found expression in the structure correlation principle[5], an inherent assumption of which is "that the interaction energy between the molecule or molecular fragment of interest and its various crystal or molecular environments can be regarded as a small perturbation relative to the total molecular potential energy".

Figure 3b shows the correlation observed for the two inter-sulphur distances in *6a*-thiathiophthenes, which may, by the structure correlation principle, be assumed to map the reaction coordinate for the valence isomerization reaction

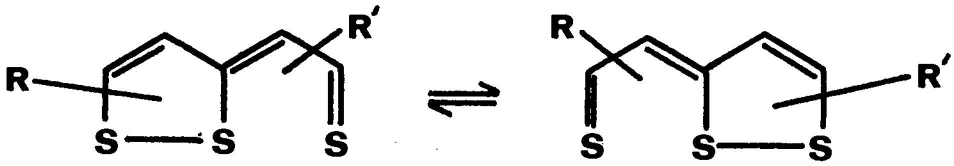

while Figure 3c maps the reaction pathway for proton transfer between a pair of oxygen atoms

OH-----O ⇌ O-----HO

in a variety of hydrogen-bonded structures.

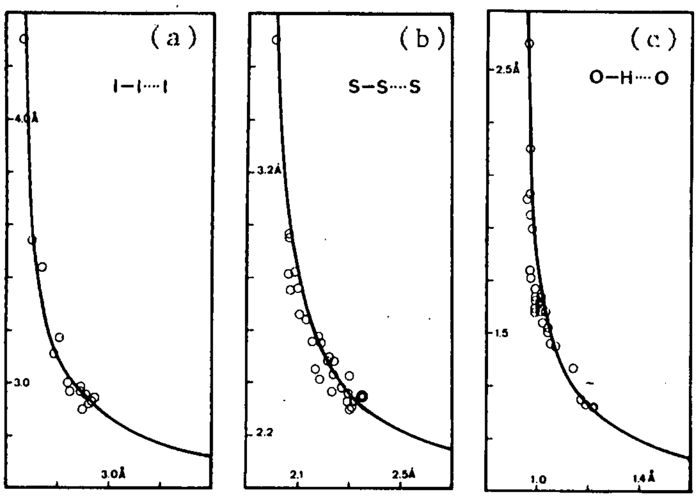

Figure 3. Correlation diagrams of interatomic distances in linear triatomic systems. (a) Triiodide anions, (b) *6a*-thiathiophthenes, and (c) hydrogen bonds. From ref.5a.

The structure correlation method hence affords one a tool whereby the gradual deformation of a molecular fragment of interest is observed through a large variety of crystalline frameworks, and is then assumed to mirror the distortion which that fragment would undergo along a given reaction coordinate. The various crystal or molecular structures hence constitute a series of "frozen in" points, or snapshots, taken along the reaction pathway, which, when viewed in the correct order, yield a cinematic film of the reaction.

APPLICATIONS OF THE PRINCIPLE

Since it was originally outlined by Bürgi[6], the structure correlation method has been used to map a number of reaction paths for substitution and addition reactions, dissociations, conformational interconversions and isomerisations. In that original communication, the first of a series of nine papers produced in partnership with Dunitz, enlarging and elaborating on the applicability of the approach, Bürgi mapped the structural pathway for the ligand-exchange reaction

$$XCdL_3 + Y \rightleftharpoons X{-}{-}{-}{-}CdL_3{-}{-}{-}{-}Y \rightleftharpoons X + CdL_3Y$$

from structural data of 11 five coordinate cadmium complexes. He showed how the data pictured the process which is believed to occur during a typical S_N2 type nucleophilic substitution reaction at a tetrahedral centre.

The approach of the attacking nucleophile (Y) at the face opposite the leaving group (X), is accompanied by the gradual flattening of the tetrahedron and a lengthening of the Cd–X bond, leading to the formation of the trigonal bipyramidal intermediate

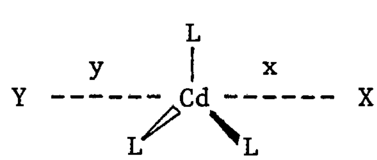

In it, Cd is coplanar with the three equatorial ligands (L), and the axial bonds x and y are equally long, but lengthened over what they would be in CdL_3Y and CdL_3X tetrahedra respectively. The axial bond distances x and y exhibit the hyperboloid relationship typical of linear three-centre, four electron systems, and can be expressed as a single function of the out-of-plane displacement (z), of Cd out of the L_3 plane, such that

$$x,y = -C\log[(\pm z + 84)/168]$$

The similarity of the above equation to that of Pauling[7], which relates changes in interatomic distances d to bond numbers n: $d = -C\log n$, leads to the conclusion that (i) z is a geometric measure of n, and (ii) the sum of the bond numbers $n_x + n_y = 1$, ie., a total bond number of 1 for the axial bonds is maintained along the reaction coordinate.

Other substitution reactions which have been mapped by the structure correlation method, are the S_N2 and a hypothetical S_N3 reaction at tetrahedral tin complexes[8]. The S_N2 pathway with inversion of configuration is shown to be very similar to that found by Bürgi[6] for cadmium, and can be analytically described by a simple expression derived from the Pauling relationship, and the assumed dependence of the bond numbers on z. Some features of the pathway for the substitution reaction with retention of configuration are also presented, but information on these is sparse, limited as it is to six fragments. Although the coordinate for a termolecular reaction, corresponding to the symmetric addition of two ligands to a tetrahedral tin moeity, may seem to be of little chemical interest, it is argued that this nevertheless corresponds to a fairly well-defined valley in the potential energy hypersurface. Moreover Britton and Dunitz suggest that such an entropically disfavoured pathway may yet turn out to be important for enzymatic reactions.

The structure correlation method has also been successfully employed in mapping the reaction coordinate for nucleophilic addition of nitrogen[9] and oxygen[10] donours to carbonyl groups. In the first case an investigation of a series of alkaloid and related structures, all containing a tertiary amino and a carbonyl group, revealed a correlation between the $R_3N.....CR_2O$ distance and the pyramidalisation (Δ) of the carbonyl group. Moreover the direction of the local threefold axis on the nitrogen, taken to represent the direction of the nitrogen lone pair, coincided within a few degrees with the N.....C direction. An *ab initio* calculation[11] of the reaction path of the simple model system

$$CH_2{=}O + H^- \rightarrow CH_3O^-$$

corresponding to the nucleophilic addition of hydride anion to formaldehyde to yield the methanolate anion, supports the results obtained from the crystal data. Figure 4 shows the correlation between the nucleophile-carbonyl distance (d) and the carbonyl group pyramidalisation (Δ) for the experimental (top curve) and for the theoretical path (bottom curve).

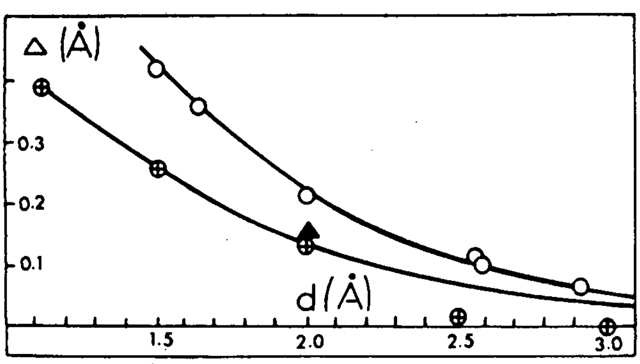

Figure 4. Plot of the pyramidalisation Δ versus the distance d between the nucleophile and the carbonyl C atom for experimental (top curve) and theoretical (bottom curve) results. From ref. 11.

An investigation of a wide variety of MX_4 and YMX_3 fragments of T_d or C_{3v} symetry (M = S,P,Al,Sn), has revealed deformations analogous to those expected for the S_N1 type of reaction, ie., they correspond to heterolytic weakening and ultimate fission of the axial bond to yield planar MX_3 species[12]. Figure 5 shows how the fragments were analyzed, and gives a scatter plot of the axial (r_2)

and the equatorial (r_1) bond lengths, corresponding to the bond undergoing rupture and the bond within the MX_3 species, versus the average angle (θ) between the axial and the equatorial bonds. It shows, that a lengthening of r_2 is accompanied by a decrease in θ, hence a flattening of the YMX_3 or MX_4 tetrahedron, and a shortening of r_1, indicating an increase in bonding in the MX_3 species, to compensate for the loss of one ligand. Interestingly, it is suggested that the Born-Oppenheimer surfaces of the molecules studied are relatively insensitive to the nature of the central atom and of the ligand.

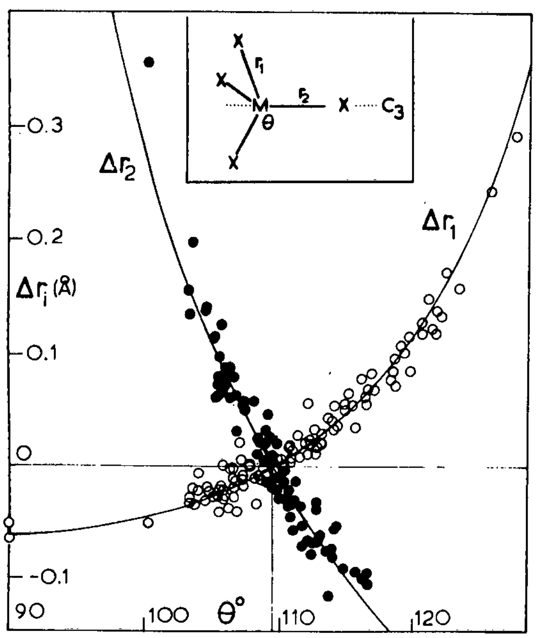

Figure 5. Correlation plot of experimental data for dissociation of a tetrahedral species. From ref. 12.

Such an insensitivity of the topography of the Born-Oppenheimer surface to the nature of the atoms constituting the fragment of interest, is also evident in two separate studies of the fluxional character of pentavalent compounds. Five-coordinate main group and transition element complexes in general exhibit trigonal bipyramidal (TBP) or square pyramidal (SQP) conformations, or some distorted form of either. In rationalizing intramolecular ligand exchange occurring in the PF_5 molecule, as evidenced by the degeneracy of the two ^{19}F n.m.r. signals at elevated temperatures, Berry[13] proposed a mechanism whereby two TBPs are interconverted via a SQP. Figure 6 outlines the now renowned Berry mechanism, which involves simultaneous in-plane bends, leading to an interchange, of the axial (1,5) and two equatorial (2,4) ligands, with the third equatorial ligand (3) acting as a "pivot" for the pseudorotation mechanism.

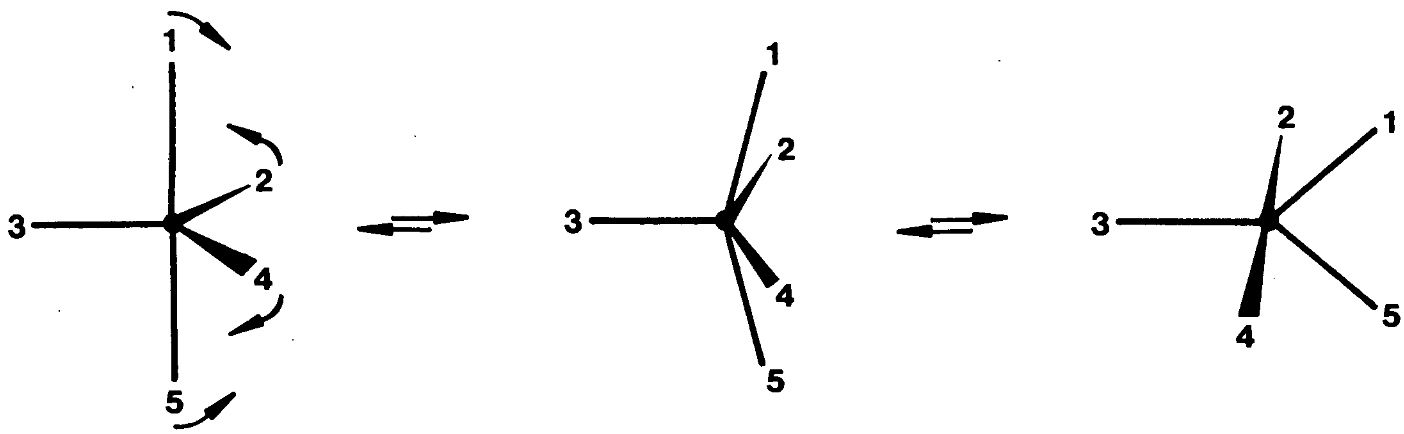

Figure 6. Diagram of the Berry mechanism.

The coordinate joining two TBPs via a SQP has been mapped from an investigation of a variety of pentavalent complexes, comprising both main group and transition elements[14], and from a systematic analysis of 34 different cyclic phosphoranes[15]. The Berry coordinate, expressed as a function of dihedral angles contained by the structures, is closely adhered to in both studies, although the scatter is more pronounced in the general study[14]. Figure 7 shows the variation of the axial angle, θ_{15}, and the equatorial angle, θ_{24}, with the dihedral angle, δ_{24}, defined by the two planes of the TBP polygon sharing the 24-edge, for the study of the phosphoranes. The solid line represents the Berry coordinate.

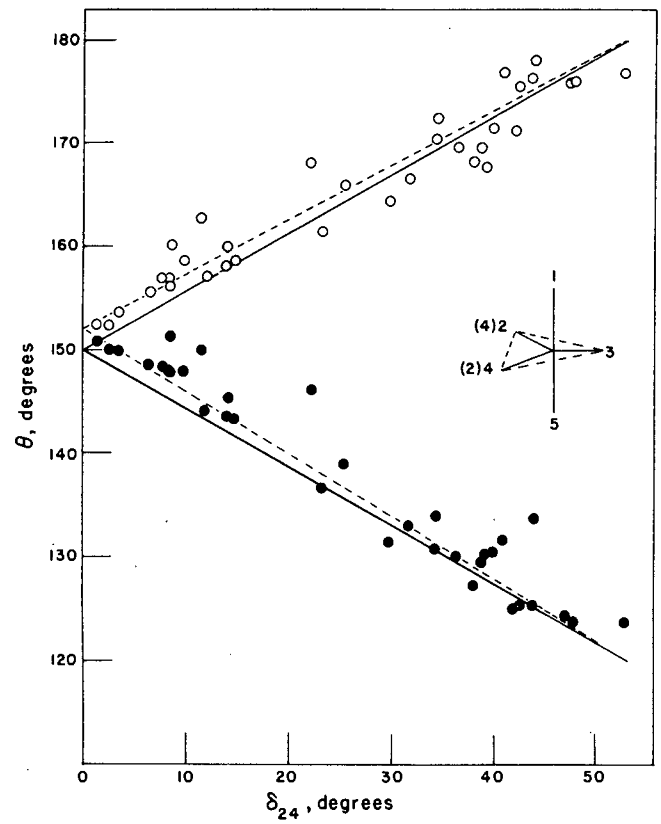

<u>Figure 7</u>. Plot of θ_{15} (open circles) and θ_{24} (closed circles) versus δ_{24} as defined in the test. Berry coordinate is the straight line. From ref. 15.

Two studies of ring closure reactions have appeared. Bürgi *et al* have mapped the reaction pathway for pericyclic 1,6-methano annulenes and related structures[16], and show that this coordinate is the path along which the angle-strain energy is kept at a minimum. Moreover they argue that the interaction between the carbon atoms undergoing bond formation is attractive all along the coordinate. Chadwick *et al* have compared the results of a structure correlation analysis of the closure of a γ-keto-acid to form a γ-hydroxylacetone

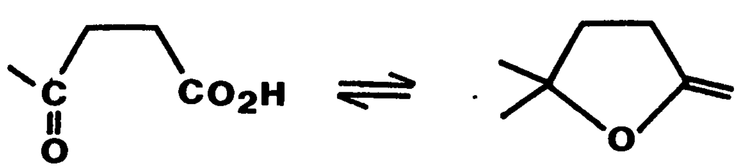

with those of an *ab initio* calculation for that reaction[17]. They have found a very close agreement between the two, and have suggested that the compounds they examined "... show signs of movement along the reaction coordinate for ring closure".

Isomerisation reactions have recently received much attention, in that four different, lengthy studies applying the structure correlation technique to such reactions have appeared within the space of one year. Hutchings[18] has examined *ortho*-substituted nitrobenzenes of the type

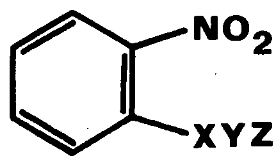

By treating the NO_2 and XYZ groups as rigid rotors, he has shown that these rotate in opposite directions, such that sum of the dihedral angles between the XYZ and NO_2 planes and the benzene ring, remains constant at 90^o. Figure 8 outlines the pathway which he has mapped.

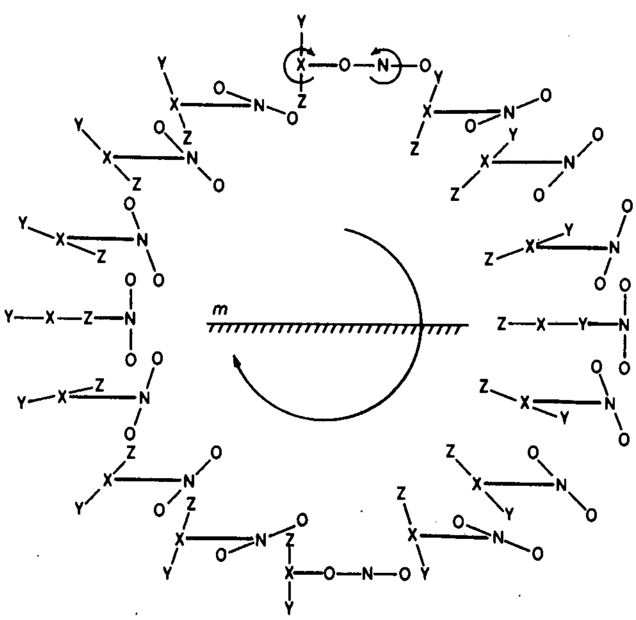

Figure 8. Pathway of isomerisation for *ortho*-substituted nitrobenzenes. The bold black line corresponds to the plane of the benzene ring. The line m represents a mirror plane, and the clockwise arrow shows the direction of the path corresponding to the disrotation shown in small arrows. From ref. 18.

In parts 8 and 9 respectively, of the series by Bürgi and Dunitz, the stereoisomerisation path for triphenylphosphine oxide[19] and a conformational interconversion of Wilkinson's catalyst[20] are examined. Using data from more than 1000 Ph_3PX fragments, the deformations of the molecule were shown to correspond to an interconversion of the form 1 and 3 via 2, by what is known as a two-ring flip mechanism.

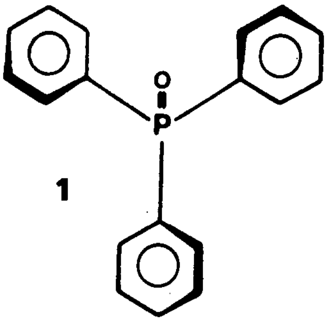

1

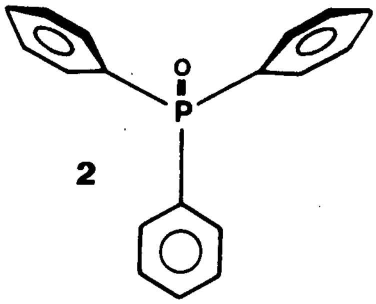

2

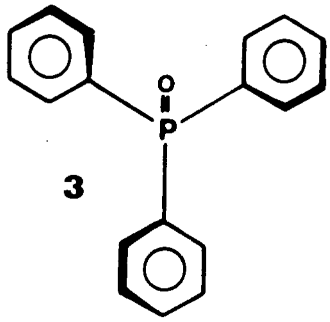

3

The analysis of Wilkinson's catalyst and 14 related molecules, based on a non-rigid molecular model of three C_{3v} - symmetric rotors PR_3 on a C_{2v} - symmetric frame XMP_3, unveiled "possible mechanisms for transmission of structural information from one side of a metal complex to the other", a finding of obvious import in studies of catalysis. A similar analysis was applied in a study[21] of the conformational dynamics of propane, di-*tert*-butylmethane and bis(9-triptycyl)methane, in which the results of empirical force field calculations are combined with those of a molecular analysis in providing a description of the internal motions of those molecules.

Finally, it appears that apart from Bürgi's study[20] on $[XM(PR_3)_3]$ and that of Muetterties on polytopal rearrangements in ML_n complexes[14], only one other study in this area on transition-metal complexes has been published. Sacconi *et al*[22] have examined the phenomenon of "ring-whizzing", a mechanism whereby a ML_n

moeity migrates about the periphery of a cyclic polyene, in complexes of the type $[(Ph_3C_3)M(PPh_3)_2]^+X^-$ where M = Ni and Pd. They have found that the results of molecular orbital calculations of the extended Hückel type closely mimic those found from a systematic analysis of the complexes.

THE AIM AND SCOPE OF THIS STUDY

Four-coordination is well established amongst the metals of the first transition series (included in that group, for the purposes of this study, is that contentious element zinc), in that nickel, copper and zinc, and cobalt less commonly, exhibit this valence. Tetra-coordination generally results in either tetrahedral or square planar conformation, or slightly distorted forms of either. Of the first transition elements, zinc exemplifies the former conformation, its four-coordinate complexes being almost exclusively tetrahedral, while nickel typically adopts a square planar geometry, as do the other metals of the nickel triad. The chemistry of such nickel compounds has, however, been largely ignored over that of platinum and palladium. Similarly "... information on substitution reactions of tetrahedral metal complexes is conspicuous largely because of its absence ...", as is pointed out by Basolo and Pearson in their authoritative work on inorganic reaction mechanisms[23].

Complexes of both types of geometry may undergo isomerisation and substitution reactions, which have been proposed to proceed via essentially similar associative mechanisms[23,24]:

$$XML_3 + Y \rightleftharpoons [XML_3Y] \rightleftharpoons X + ML_3Y \qquad (3)$$

where X,L represent any coordinated ligand atoms, Y is either X,L or solvent, and M = Ni, Zn. The rate of this reaction may be determined by either the associative or the dissociative step, or a combination of both. The nature of the five coordinate intermediate has been the subject of much discussion, with suggestions[23] that it has a trigonal bipyramidal conformation for both metals, or a square pyramidal one for nickel[24]. Moreover it has been postulated, and in many cases shown, that this intermediate $[XML_3Y]$ may exhibit the fluxional behaviour typical of many penta-coordinate compounds, and best described by the Berry mechanism, shown in Figure 6.

This study applies the principle of structure correlation analysis to five coordinated nickel and zinc complexes $[ML_5]$. The results are viewed as mapping reaction coordinates for association reactions at square planar nickel and tetrahedral zinc centres, resulting in five coordinate intermediates, with subsequent pseudorotation and dissociation of these.

DATA SEARCH AND STRUCTURE ANALYSIS

The Cambridge Crystallographic Data Centre (CCDC) file contains information of the space group and positional atomic coordinates for all organic and organometallic crystal structures published[25]. This file was searched for compounds containing both nickel and zinc, with at least four non-hydrogen atoms bonded to the metal. The data retrieved were then similarly treated for both groups of compounds.

ZINC

A search of the CCDC file (January 1983 edition) revealed 379 entries, of which 53 were considered five-coordinate, with the ligand atoms at a distance of not more than 100 pm in excess of the sum of the covalent radii of the relevant atoms. After rejecting allyl complexes (for lack of definite atoms of ligation) and porphyrin complexes (because of the ligands' steric constraints), the remaining 33 different entries corresponded to 34 different arrangements, one compound (identified by the CCDC acronym-ZNIPXT[26]) being a dimer with two crystallographically distinct zinc atoms. In all cases the metal was considered to be in the 2+ oxidation state. Figure 9 shows the structural formulae of the compounds.

NICKEL

A search of the March 1983 edition of the CCDC file (containing 31982 entries) for nickel containing compounds revealed 1135 structures. After the process of elimination 72 different five-coordinate complexes were identified, corresponding to 78 distinct

Figure 9. Molecular structures of the zinc compounds used. Percentage distortion TBP → SQP is given in parenthesis behind the compound number.

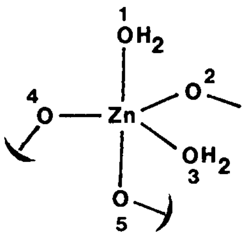

1 (28)

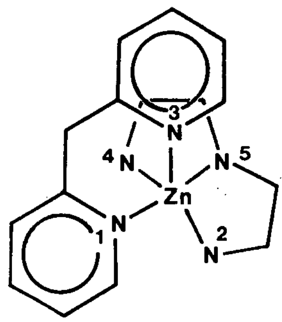

2 (37)

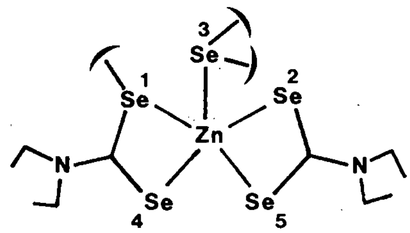

8 (56)

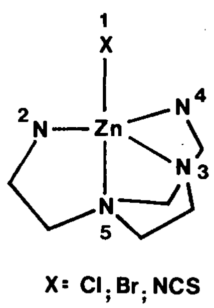

3,7,23 (24,20,28)

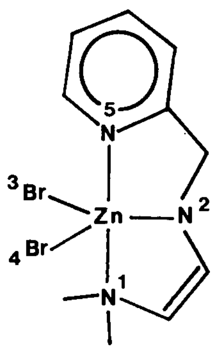

4 (56)

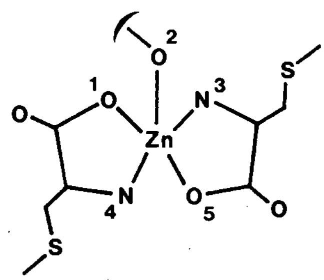

10 (19)

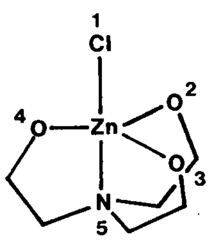

5 (26)

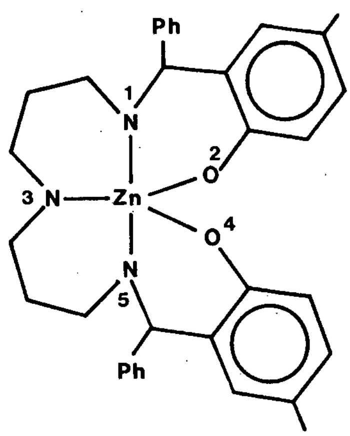

6,11 (14,15)

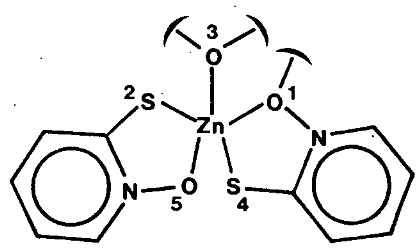

14,15 (32,31)

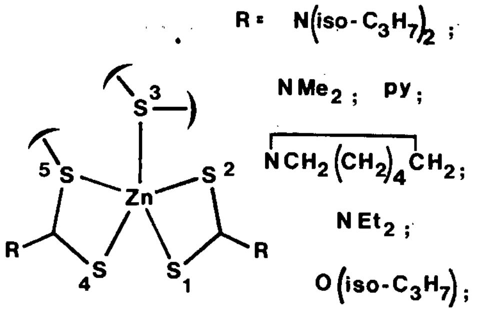

9,12,16,18,19,21a,21b
(62,61,59,57,58,20,61)

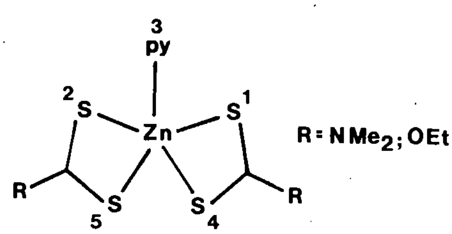

13,25 (26,61)

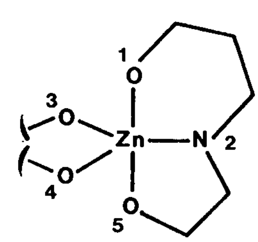

17 (54)

Figure 9. (continued)

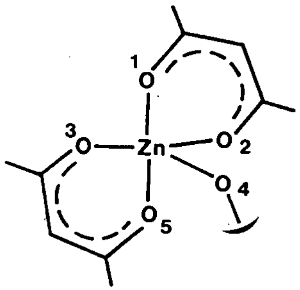

20 (18)

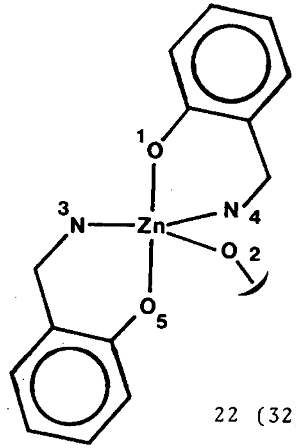

22 (32)

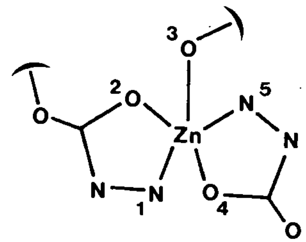

29 (90)

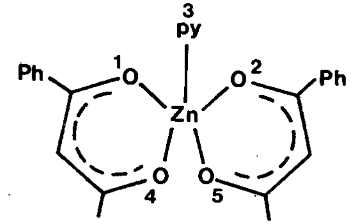

30 (82)

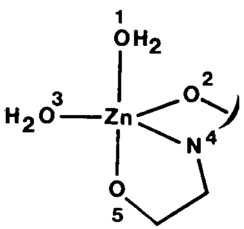

24 (34)

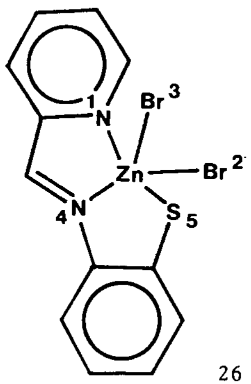

26 (58)

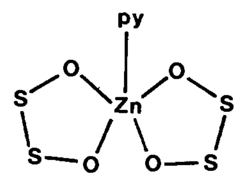

31 (98)

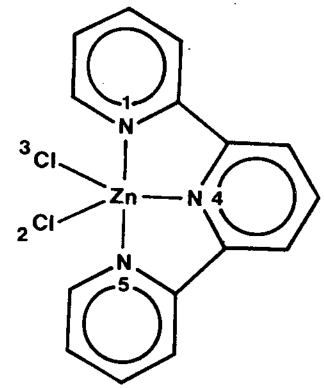

32 (65)

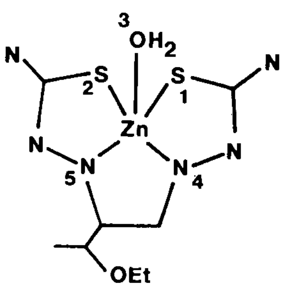

27 (74)

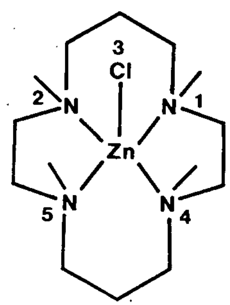

28 (91)

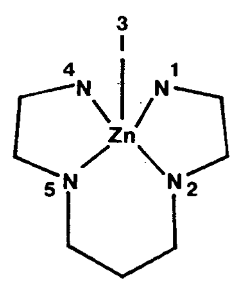

33 (74)

Figure 10. Molecular structures of some nickel compounds of special interest.

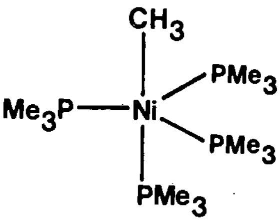

BAPKEI

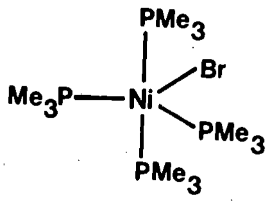

BMPNIB 1Ø

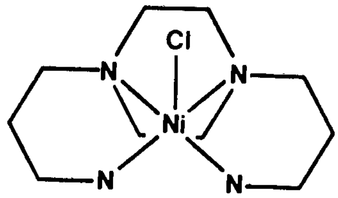

CAPPNC

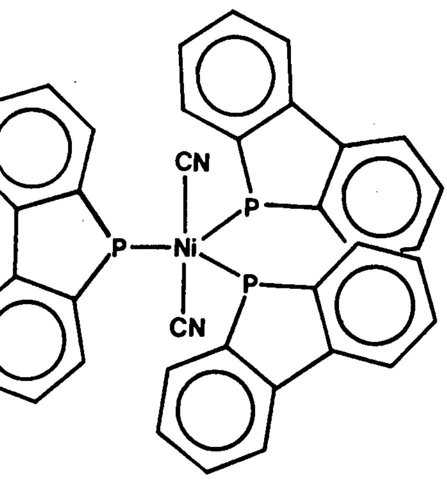

CMPNIM

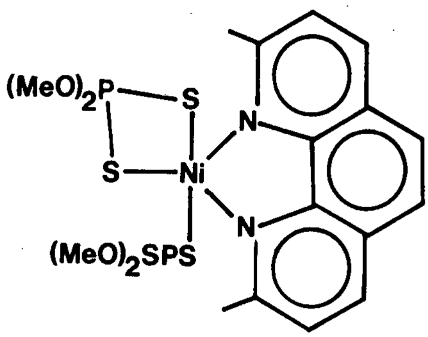

DMPADP 1Ø

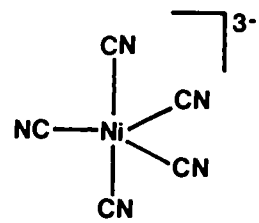

EDCRCN

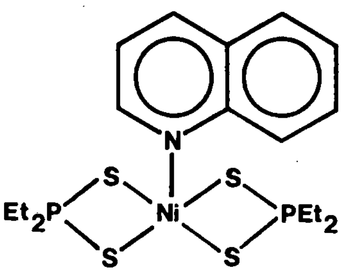

ESPNIQ

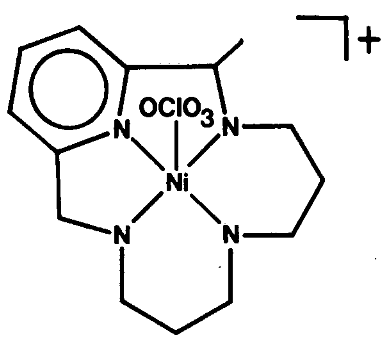

MAZNIP

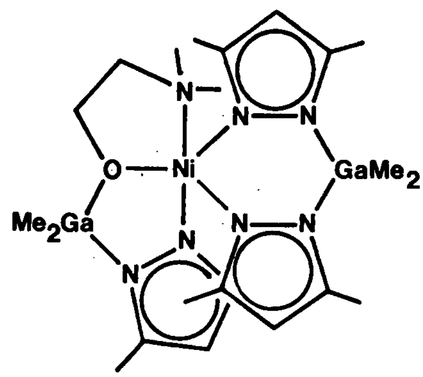

MPGANI

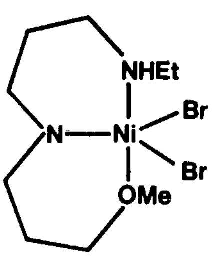

MOPAON

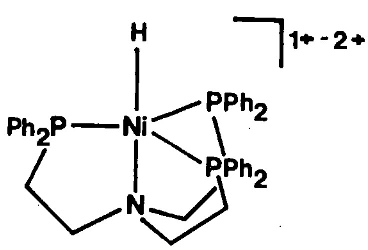

NIHNPB

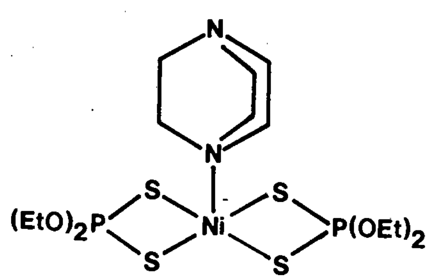

TEDTEP

arrangements of the ligand donor atoms about the nickel, which, in general, was in the 2+ oxidation state.

A cursory examination of both the nickel and the zinc complexes revealed large variations in ligand to metal distances, and a spectrum of conformations ranging from trigonal bipyramidal (TBP) to square pyramidal (SQP). Interestingly two complexes, dicyanotris-(5-methyl-5H-dibenzophosphole)nickel(II) (CCDC acronym = CMPNIM)[27] and the pentacyano-nickelate(II) anion (EDCRCN)[28] adopt both distorted TBP and SQP conformation. Their structural formulae are shown in Figure 10.

The molecular geometries of the ML_5 fragments were analysed as shown in Figure 11. In order to put all distances on a common scale, the sums of the respective covalent radii of the metal and the ligand donor atoms D_i (i = 1,2,3,4,5) were substracted from the actual inter-atomic distances to yield distance increments d_i. The covalent radii used (in pm) were Zn(131), Ni(121), C(77), N(70), O(66), P(110), S(104), Cl(99), As(121), Se(117), Br(114), Sn(140) and I(133), all after Pauling[29].

Ligand donour atoms D_1 and D_5 were identified as containing the largest bond angle θ_{15}, with D_1 fulfilling the following requirements best: (i) $d_1 < d_5$, (ii) D_1 is a better leaving group and (iii) the metal atom is displaced towards D_1. D_2 and D_4 were then in general defined by the next largest contained angle θ_{24}, thus in turn defining D_3. Two further parameters were also determined, these being the out-of-plane displacements z and x. The former was defined as the displacement of the metal out of the equatorial plane defined by D_2, D_3 and D_4 in the TBP. The latter is the distance between the metal and the basal plane defined by D_1, D_2, D_4 and D_5 in the SQP. Table 1 and Table 2 list the distance increments, atom types and displacements for the zinc and nickel complexes respectively, while appendix 1. lists the corresponding bond angles θ_{ij}.

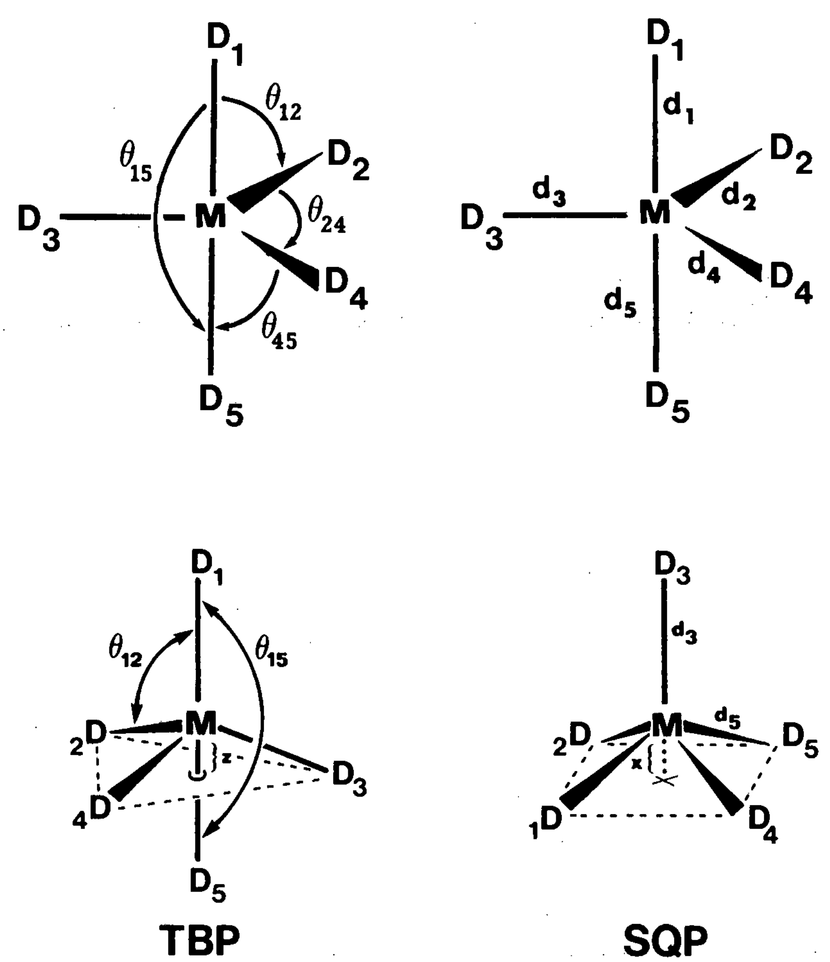

Figure 11. Diagram of molecular geometries showing distance increments d_i, bond angles θ_{ij} and displacements x and z. (M = Ni,Zn).

In order to define the conformations of the fragments more rigorously than simply as "distorted SQP" or "distorted TBP", the dihedral angle method of Muetterties and Guggenberger[14] was employed. This method relies on the changes in the nine dihedral angles which are defined in an ideal TBP as it distorts towards a SQP via the Berry mechanism. The dihedral angles (δ_{ij}) are defined by the angles between the normals to the planes sharing a common edge (ij) in the idealised polyhedra as shown in Figure 12. By relating the dihedral angles of the compounds under consideration to those in the idealised structures their amount of distortion may be calculated. This is also presented in Tables 1 and 2. Table 3 lists the θ_{ij} and δ_{ij} values for the idealised conformations which were chosen, as well as the absolute changes $|\Delta|_{ij}$.

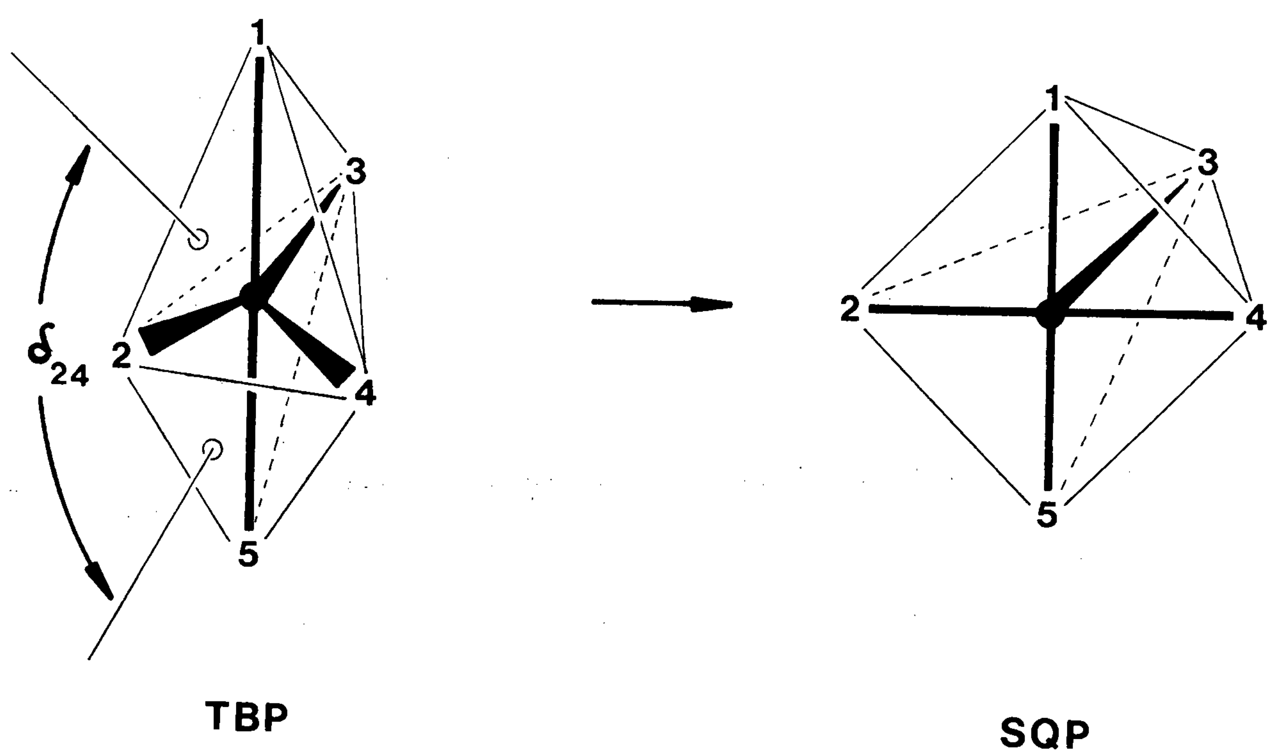

Figure 12. Diagram showing dihedral angles and edges in the idealised polyhedra.

The model SQP was chosen as having apical-basal bond angles (θ_{31}, θ_{32}, θ_{34}, θ_{35}) of 105^{o}. This is the configuration obtained by placing M at the centre of mass of a ML_5 square pyramid, and is the same as that chosen by Holmes[15]. Appendix 1. also lists the dihedral angles for the compounds under consideration.

Table 1. CCDC acronyms, atom types, distance increments d/pm, displacements z/pm and x/pm for TBP and SQP respectively and percentage distortion from TBP → SQP for the zinc compounds.

mpd. o.	CCDC Acronym	D_1	D_2	D_3	D_4	D_5	d_1	d_2	d_3	d_4	d_5	z	x	%
1	ACBZNM	O	O	O	O	O	13	6	2	1	14	−1	41	28
2	AEPYZN	N	N	N	N	N	14	9	7	7	24	9	56	37
3	AEZNPB	Cl	N	N	N	N	1	5	6	5	32	39	50	24
4	BPAZHZ	N	N	Br	Br	N	23	8	−1	−2	23	4	64	56
5	CEANZN	Cl	O	O	O	N	−3	15	4	13	14	32	57	26
6	CPZHZN	N	O	N	O	N	11	−2	15	−3	11	2	41	14
7	DAEAZN	Br	N	N	N	N	3	11	11	11	19	27	52	20
8	ESECZN	Se	Se	Se	Se	Se	9	−3	1	−4	55	25	68	56
9	IPTCZN	S	S	S	S	S	11	−1	3	−1	47	23	69	62
0	MCYSZN	O	N	O	N	O	12	3	1	8	16	5	39	19
1	MPZHZN	N	O	N	O	N	10	−1	−2	18	10	4	40	15
2	MTCAZN	S	S	S	S	S	8	−2	2	−4	69	35	63	61
3	MTCPZB	S	S	N	S	S	25	−1	7	−2	26	2	63	26
4	OXPTZN	O	S	O	S	O	8	−4	15	−4	21	8	32	32
5	OXPZND	O	S	O	S	O	8	−3	12	−4	22	11	35	31
6	PCDTZN 1Ø	S	S	S	S	S	14	−3	3	−1	56	27	69	59
7	SALEZN	O	N	O	O	O	−3	0	2	3	45	44	46	54
8	XMTCZN	S	S	S	S	S	9	0	−1	−1	61	31	78	57
9	ZETCAM	S	S	S	S	S	9	1	3	−2	47	21	63	58
0	ZNACAT 1Ø	O	O	O	O	O	3	0	4	8	13	19	47	18
1a	ZNIPXT	S	S	S	S	S	6	0	−4	−1	80	43	29	20
1b		S	S	S	S	S	2	−1	−4	1	93	49	95	61
2	ZNMSAL 1Ø	O	N	N	O	O	0	6	4	3	13	17	51	32
3	ZNTATE 1Ø	N	N	N	N	N	3	6	4	5	28	33	53	28
4	GLYZNS 1Ø	O	N	O	O	O	16	2	1	−1	22	5	35	34
5	EXAPYZ	S	S	N	S	S	40	−6	2	−6	40	0	82	61
6	MTPYMZ	N	Br	Br	N	S	14	−2	−4	11	29	11	72	58
7	BTCBZN	S	S	O	N	N	1	1	12	12	14	38	41	74
8	CTAZZN	N	N	Cl	N	N	18	20	−3	18	19	3	54	91
9	HYZCZN	N	O	O	O	N	7	9	6	6	7	3	46	90
0	NZBAAE 1Ø	O	O	N	O	N	0	−3	7	7	10	6	54	82
1	PYZNDT	O	O	N	O	O	4	4	4	4	4	3	47	98
2	TPYZNC Ø1	N	N	Cl	Cl	N	17	8	−2	−4	24	1	56	65
3	ZNETAM 1Ø	N	N	I	N	N	12	16	−5	13	20	16	71	74

Table 2. CCDC acronyms, atom types, distance increments d/pm, displacements z/pm and x/pm for TBP and SQP respectively, percentage distortion (%) from TBP SQP, charge on the metal (q) and spin state (S)(as far as it has been reported) for the nickel compounds.

No.	CCDC Acronym	D_1	D_2	D_3	D_4	D_5	d_1	d_2	d_3	d_4	d_5	x	z	%	S	q
1	PEACNI 1Ø	C	P	P	P	N	10	-1	-7	-10	54	54	25	21		2
2	BACBEM	P	P	Br	P	P	-8	-7	39	-9	-8	28	5	78		2
3	BGLNIA 1Øa)	N	N	N	N	N	-4	-5	81	-5	-3	12	1	86	L	2
4	BGLNIA 1Øb)	N	N	N	N	N	-4	-4	69	-4	-3	14	0	86	L	2
5	BIQNIQ	Cl	Cl	N	N	Cl	11	17	13	13	20	37	10	71		2
6	MPNBNI	Br	N	N	Br	Br	11	12	11	12	30	34	17	54		2
7	MPNCNI	Cl	N	N	Cl	Cl	11	14	12	18	22	34	10	69		2
8	BPPENI	Br	P	Br	P	N	-2	-14	35	-14	9	17	0	90	L	2
9	BPYRNI	N	N	N	N	N	-7	-6	44	-6	-7	20	0	93	L	2
10	BTCYTN	S	S	S	S	S	-8	-1	16	-8	-2	31	13	81		3
11	CAPPNC	N	N	Cl	N	N	14	14	43	20	19	34	16	91		2
12	CMPNIM b)	P	C	P	C	P	-13	-11	1	-13	-13	50	0	59		2
13	CMPNMI	N	Cl	N	Cl	Cl	12	12	5	12	26	41	5	57		2
14	CPHENI	Cl	N	N	Cl	Cl	12	16	15	19	18	39	6	81		2
15	CRTNCN Ø1a)	C	C	C	C	C	-9	-11	18	-11	-7	30	0	97		2
16	CRTNCN Ø1b)	C	C	C	C	C	-10	-11	12	-12	-8	33	-2	97		2
17	CYPSNI	N	N	I	N	N	-4	-5	30	-1	-4	24	1	83	L	2
18	DMPADP 1Ø	S	N	N	S	S	17	12	6	5	33	42	11	53		2
19	ESPNIQ	S	S	N	S	S	17	16	15	14	17	52	2	83		2
20	DPENIA	I	As	As	As	N	32	-6	-7	-6	56	59	34	14		1
21	DPENIB	I	P	P	P	N	48	-2	-5	-5	35	59	23	15		1
22	EDCRCN a)	C	C	C	C	C	-11	-11	19	-14	-11	33	0	95		2
23	INOPNI	I	P	O	P	N	-6	-11	75	-10	8	12	0	76	L	2
24	IPBNIB	N	N	Br	N	N	1	-3	31	0	-3	24	1	88	L	2
25	MASONI 1Ø	O	O	O	O	O	13	13	7	13	14	39	-4	84		2
26	MAZNIP	N	N	O	N	N	-9	4	91	4	4	12	-21	74		2
27	MOPAON	N	Br	N	Br	N	10	7	11	5	41	35	16	69		2
28	MPGANI	N	O	N	N	N	15	11	9	9	32	49	6	35		2
29	MTZNIT	N	N	N	N	N	14	15	11	8	19	27	4	70		2
30	NBOSNI	S	S	S	S	S	-11	-9	103	-8	-10	13	-7	83		2
31	NICEAS 1Ø	O	O	N	N	N	6	8	7	29	9	36	4	85		2
32	NIDSPI	I	S	S	I	P	3	-6	54	-3	-19	10	7	91	L	2
33	NIPPNS	S	P	P	P	N	11	-5	-6	-6	36	55	24	9		0
34	PEMENI	N	P	O	P	N	-6	-10	61	-10	5	14	13	89	L	2
35	PHASNI	P	As	As	As	N	4	-2	-1	0	68	58	46	7		1
36	PMENSE	P	O	P	P	O	3	14	-1	5	12	40	14	82	H	2

Table 2. (continued)

No.	CCDC Acronym	D_1	D_2	D_3	D_4	D_5	d_1	d_2	d_3	d_4	d_5	x	z	%	S	q
37	PTNNIB 10	P	P	I	S	S	-9	-13	11	1	-1	26	11	88		2
38	PYEENI	N	N	N	N	N	19	17	10	15	21	33	3	94	H	2
39	QUMQNI	Cl	N	N	Cl	Cl	10	14	15	20	23	41	5	93	H	2
40	TCAPAN 10	N	N	N	N	N	6	31	4	26	17	34	20	99	H	2
41	TEDTEP	S	S	N	S	S	19	18	22	19	20	54	0	95		2
42	TPIVNI	S	S	S	S	S	-4	-4	46	-3	-2	20	0	93		2
43	TMCAZN	N	N	N	N	N	19	20	4	19	20	33	4	97		2
44	ASPHNI	P	As	As	As	C	-10	-11	-8	-11	-9	59	19	13		2
45	ATSZNI	N	S	Cl	S	N	15	6	9	6	15	43	1	22	H	2
46	AZOCNI	N	Cl	Cl	Cl	N	24	10	8	11	25	60	1	9	H	2
47	BAPKEI	P	P	P	P	C	-10	-5	-6	-5	6	55	24	21	L	2
48	BEBPNI	P	Br	P	Br	P	-8	16	-13	11	-9	78	4	11		2
49	BMPANI	N	Br	N	Br	N	14	14	10	12	14	19	1	39	H	2
50	BMPNIB 10	P	Br	P	P	P	-6	16	-2	-5	-6	61	1	22	L	2
51	BMPONI	P	Br	P	P	P	-13	11	-7	-12	-13	58	0	12		2
52	CEBPNI	C	P	P	P	C	-16	-7	-4	-6	-13	53	3	21	L	2
53	CMPNIM a)	C	P	P	P	C	-12	-9	-2	-8	-11	47	3	26		2
54	CMTPPN	Cl	S	S	S	P	3	-1	2	4	-20	51	6	15		2
55	CNTPNI	C	P	P	P	C	-12	-9	-5	-9	-14	52	2	22		2
56	CPEANI	Cl	P	P	P	N	-3	-12	-1	-9	6	51	9	16	L	2
57	CPEPNI	C	P	P	P	C	-11	-10	-2	-12	-9	51	0	30		2
58	DIPHNI 10	I	P	P	P	N	17	-9	-9	-9	22	56	1	7	L	2
59	EDCRCN b)	C	C	C	C	C	-15	-7	1	-8	-13	37	0	41		2
60	ETBPNI	P	Cl	P	Cl	P	-10	15	-12	15	-10	77	1	8		2
61	IMPCNI	P	I	I	C	P	-9	7	7	-25	-8	47	0	9		2
62	IMPONI	P	I	I	P	P	-12	12	12	-14	-12	56	5	14		2
63	INPNII	I	P	N	P	N	1	-5	39	-10	12	46	13	27	L	2
64	MTRENI 10	N	N	N	N	N	6	23	16	18	13	48	19	15		2
65	NIEACL 10	O	N	N	O	N	11	26	25	10	18	62	19	24		2
66	NIHNPB	H	P	P	P	N	6	-10	-10	11	15	62	4	17		1~2
67	OXPHAD	P	P	P	P	P	-17	-11	-15	-10	-16	54	0	8		2
68	PASNIB 10	C	As	As	As	N	-10	-10	-3	-12	19	61	16	17		2
69	PEAMNI	C	P	P	P	N	4	-9	-6	-8	20	55	11	10		2
70	PEASNI	S	P	P	P	N	-12	-3	3	2	16	54	12	12		2
71	PSNPEA 10a)	Sn	P	P	P	N	-7	-2	-1	-4	26	54	18	8		2
72	PSNPEA 10b)	Sn	P	P	P	N	-4	-1	-7	-2	7	61	12	16		2
73	SALDNI	N	O	N	O	N	12	14	15	11	12	31	7	47		2
74	SAIMNI 10	N	O	N	O	N	8	8	17	8	10	36	0	38		2
75	TMPBNI a)	P	Br	Br	P	P	-10	7	23	-11	-10	40	0	16		2

Table 2. (continued)

No.	CCDC Acronym	D_1	D_2	D_3	D_4	D_5	d_1	d_2	d_3	d_4	d_5	x	z	%	S	q
76	TMPBNI b)	P	Br	Br	P	P	-10	11	20	-12	-10	39	0	19		2
77	TPENIB 1Ø	S	P	P	P	P	1	-7	-2	-1	-15	52	20	18	L	2
78	IPESNI	P	I	I	S	P	-12	0	25	-6	-12	37	4	36		2

Table 3. Bond angles θ and corresponding dihedral angles δ for the idealised TBP and SQP conformations.

	θ_{15}	θ_{12}	θ_{13}	θ_{14}	θ_{52}	θ_{53}	θ_{54}	θ_{23}	θ_{24}	θ_{34}
TBP	180	90	90	90	90	90	90	120	120	120
SQP	150	86	105	86	86	105	86	105	150	105
$\|\Delta\|_{ij}$	30	4	15	4	4	15	4	15	30	15
$\sum_{ij}\|\Delta\|_{ij}$					136					

	δ_{45}	δ_{25}	δ_{14}	δ_{12}	δ_{35}	δ_{13}	δ_{23}	δ_{34}	δ_{24}
TBP	101.5	101.5	101.5	101.5	101.5	101.5	53.1	53.1	53.1
SQP	118.5	118.5	118.5	118.5	76.9	76.9	76.9	76.9	0
$\|\Delta\|_{ij}$	17	17	17	17	24.6	24.6	23.8	23.8	53.1
$\sum_{ij}\|\Delta\|_{ij}$					217.9				

CORRELATIONS AND REACTION PATHWAYS

SUBSTITUTION REACTIONS AT ZINC

(i) Berry Pseudorotation

The large range of conformations which the zinc complexes exhibit already hints at the existence of a Berry coordinate, which we map using the dihedral angle method previously employed by Muetterties, Guggenberger[14] and Holmes[15].

Table 3 shows that the sum, over all edges, of the changes in dihedral angles accompanying the TBP → SQP transition is $\Sigma_{ij} |\Delta_{ij}| = \Sigma_{ij} |\delta_{ij}(TBP) - \delta_{ij}(SQP)| = 217,9^{o}$. If a compound C lies on the Berry rearrangement coordinate between TBP and SQP then its dihedral angles, $\delta_{ij}(C)$ are related to those of the idealised structures such that the sum of $\Sigma_{ij}|\delta_{ij}(C) - \delta_{ij}(TBP)|$ and $\Sigma_{ij}|\delta_{ij}(C) - \delta_{ij}(SQP)|$ is $217,9^{o}$. Figure 13 shows a plot of $217,9 - \Sigma_{ij}|\delta_{ij}(C) - \delta_{ij}(SQP)|$ versus $\Sigma_{ij}|\delta_{ij}(C) - \delta_{ij}(TBP)|$, with the Berry coordinate shown as the straight line of unit slope going through the origin. The scatter of the points from the coordinate may indicate the distortion of the compound geometries from the minimum energy path associated with the Berry mechanism. It must be recognised however, that whereas the geometry of the TBP and its associated dihedral angles are fixed, this is not the case for the SQP. The values of the SQP dihedral angles are dependent on the apical-basal angle chosen and the scatter of the points in Figure 13 will also depend on this.

The turnstile coordinate has been postulated as an alternative mechanism for describing intramolecular ligand exchange in five coordinate complexes[30]. It involves an internal rotation of one apical and one equatorial ligand, rotating as a pair, and the opposite rotation of the three remaining ligands. Whereas the Berry coordinate ideally involves the interchange of two D_{3h} TBPs via a C_{4v} SQP, the turnstile coordinate involves three intermediates of C_s symmetry.

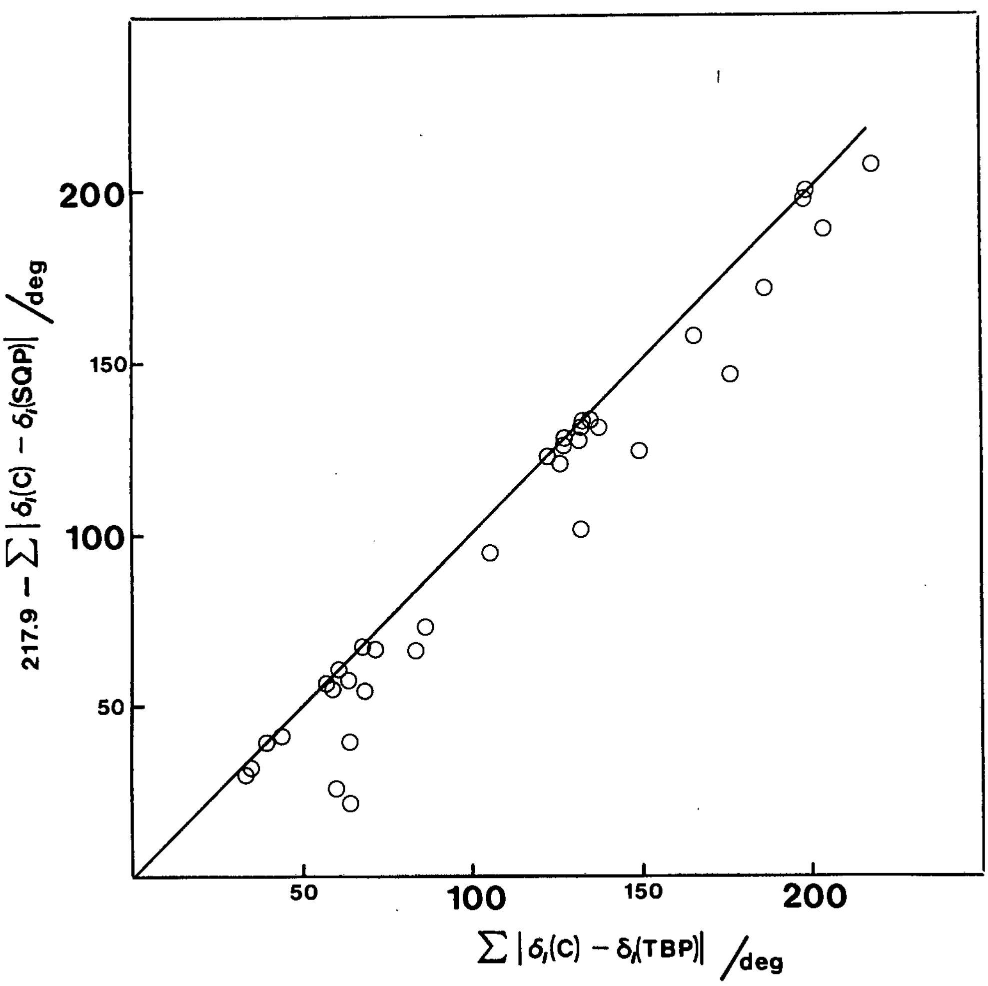

Figure 13. Plot showing adherence of Zn compounds to the Berry coordinate represented by the straight line.

Two independent *ab initio* examinations, one[31] on the model compound PH_5, and the other[32] on PF_5, have shown however that the latter mechanism requires a considerably higher activation energy and is not a strictly different mechanistic pathway, but can be regarded as a distortion of the penta-coordinate moiety away from the minimum energy path of the Berry process. Both studies conclude that a turnstile representation will only be realised for structurally restricted systems and the true saddle point in the interconversion of the two trigonal bipyramids corresponds to the square pyramidal intermediate with C_{4v} symmetry. We surmise that the distortions away from the Berry coordinate, as shown by some points in Figure 13 are possibly towards a 'turnstile coordinate', and that these are brought about by a combination of structural restrictions imposed by the ligands.

Favas and Kepert[33] have calculated the potential energy hyper-surface for a pentacoordinate system [M(unidentate)$_5$]. This maps the reaction coordinate for the interconversions between a trigonal bipyramid T_0 and two other trigonal bipyramids T_1 and T_2 via square pyramidal intermediates S_1 and S_2. These conformations are shown in Figure 14.

In their study Favas and Kepert define an axis (as shown in Figure 14) in each of the structures T_0, T_1, T_2, S_1 and S_2 such that the angles ϕ_A, ϕ_B, and ϕ_C between this axis and the bonds to each of the atoms A, B and C, are all equal. ϕ_D and ϕ_E are then the angles found between the axis and the bonds to D and E respectively. Figure 15 shows the projection of the potential energy surface onto the ϕ_D - ϕ_E plane, and is reproduced from that study. The surface is symmetrical across the line $\phi_E = 180^\circ - \phi_D$.

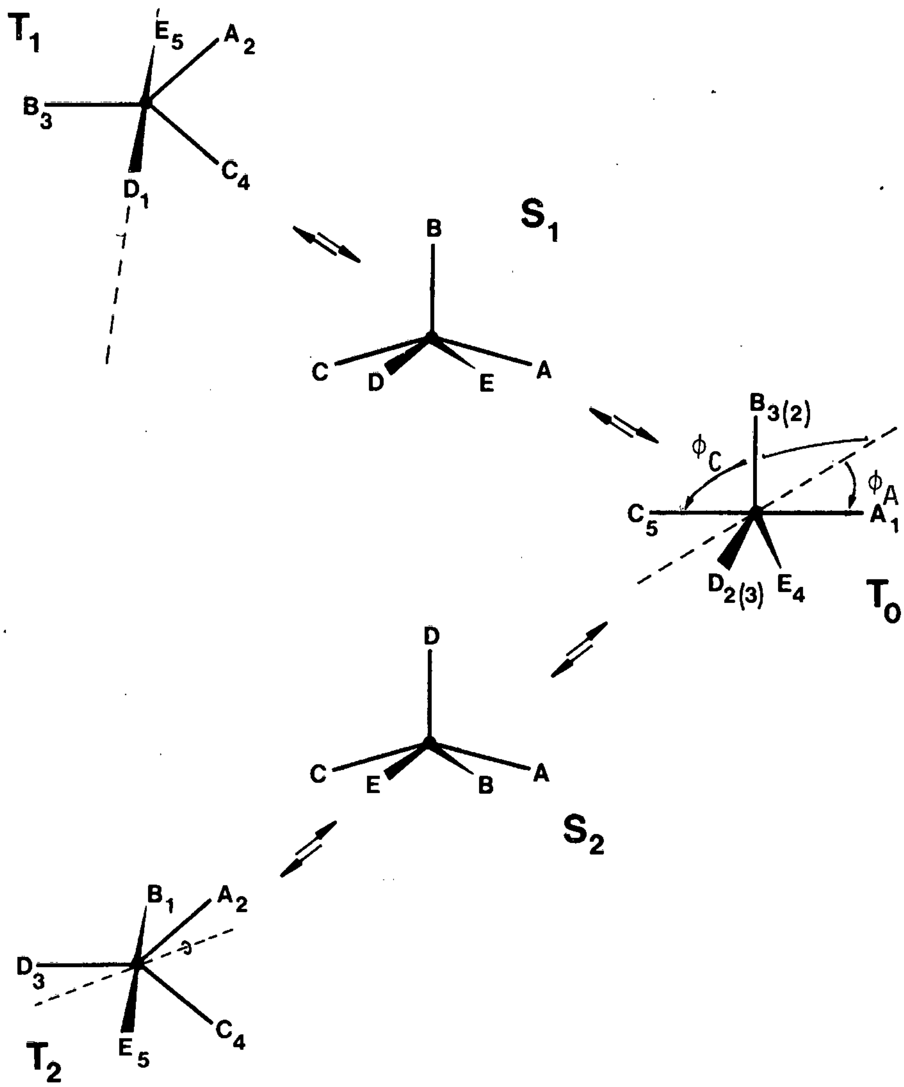

Figure 14. Diagram showing conformations of T_0, T_1, T_2, S_1, S_2 and interconversions between them. Numbers show our superimposed numbering system. Adapted from ref. 33.

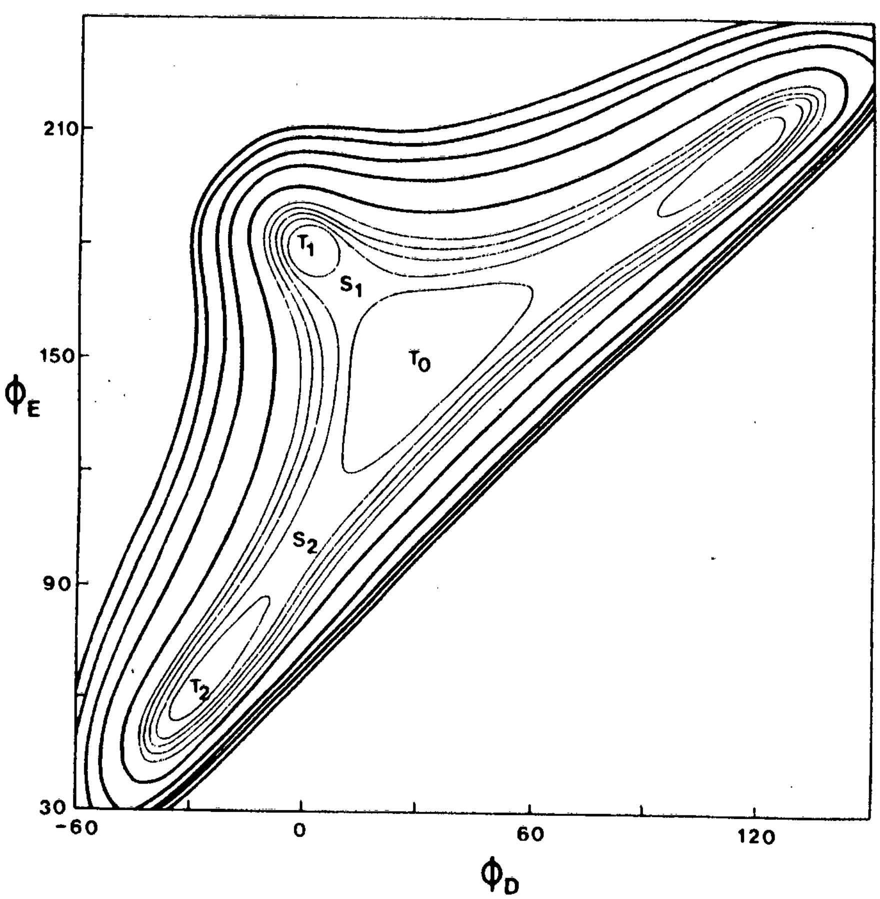

Figure 15. Potential energy surface for system shown in fig. 14. From ref. 33.

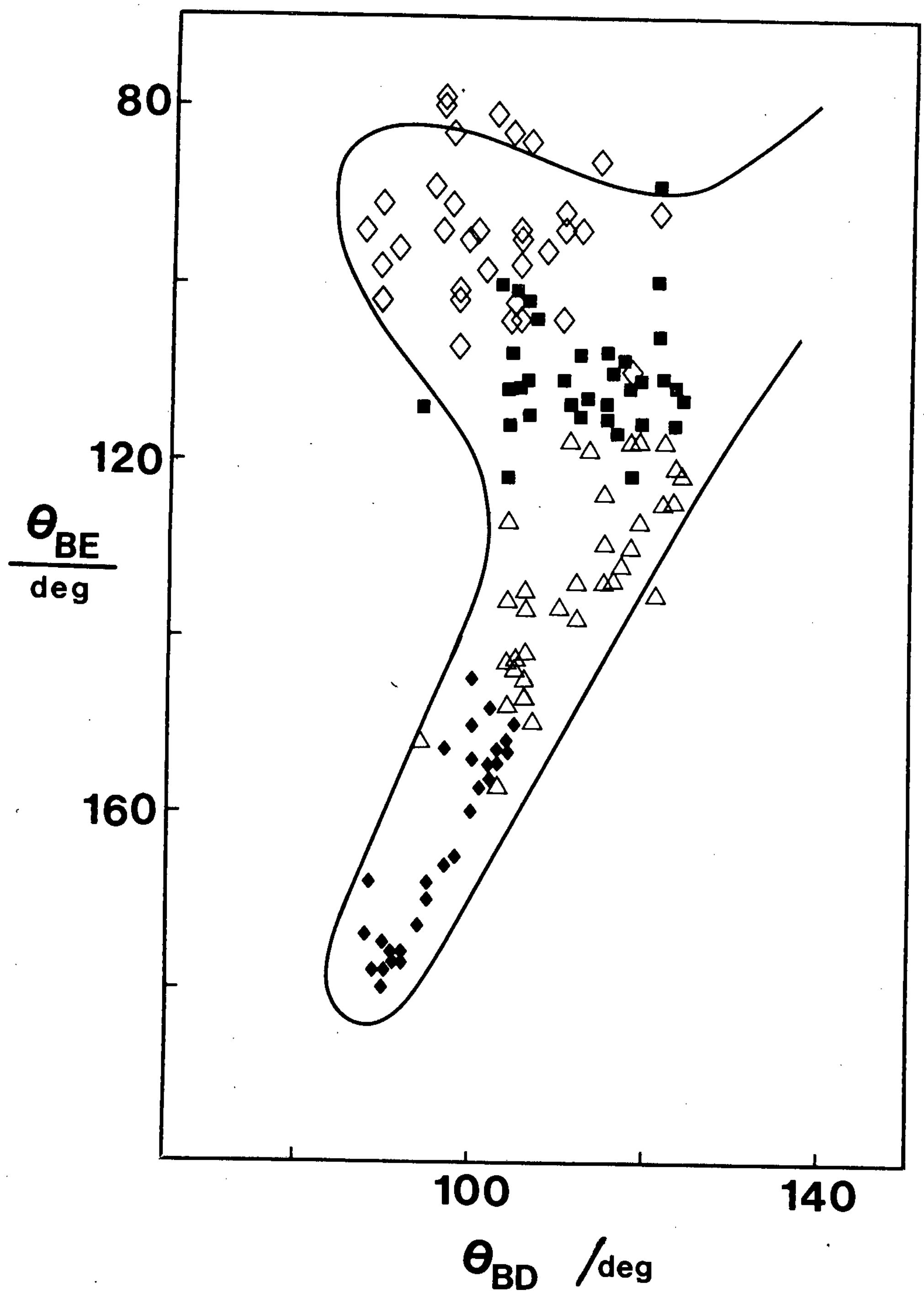

Figure 16. Plot of structural data for zinc compounds onto the surface defined by θ_{BE} and θ_{BD}.

For the purposes of comparison we regarded the ligands as identical and unidentate, thus reducing the 34 different arrangements to the common system $[ZnL_5]$. Noting that the angles ϕ_D and ϕ_E are defined within the plane BDE, we chose to project the reaction coordinate derived from the crystal structures onto that plane, by plotting θ_{BD} against θ_{BE}. By superimposing our choice of ligand numbering on the conformations T_0, T_1 and T_2 (as is shown in Figure 14) the parameters θ_{BE} and θ_{BD} were calculated and plotted on Figure 16. The similarity between the point charge model and that obtained from the crystal structures is gratifying.

The foregoing discussion has shown the possibility of the five coordinate zinc complex undergoing pseudorotation. Recalling that the TBP conformation may represent the intermediate in the S_N2 mechanism:

$$D_5 + L_3ZnD_1 \rightarrow [D_5 \ldots . ZnL_3 \ldots . D_1] \rightarrow D_5ZnL_3 + D_1$$

where L = D_2, D_3, D_4, we wished to further characterise this intermediate.

The distortions which arise in the complexes as the entering nucleophile D_5 approaches the zinc ion are tabulated in Table 1 and shown on Figure 17.

The plot of d_5 vs % distortion from TBP to SQP shows that for $d_5 > 30$ pm the conformation of the $D_5 \ldots . L_3ZnD_1$ system is displaced approximately 57% towards SQP. Structure 21a (d_5 = 80 pm, 20%) is distorted from the mean line of attack by the close presence of a sixth potential donor ligand. The geometry of this structure also lies furthest away from the Berry coordinate shown in Figure 13.

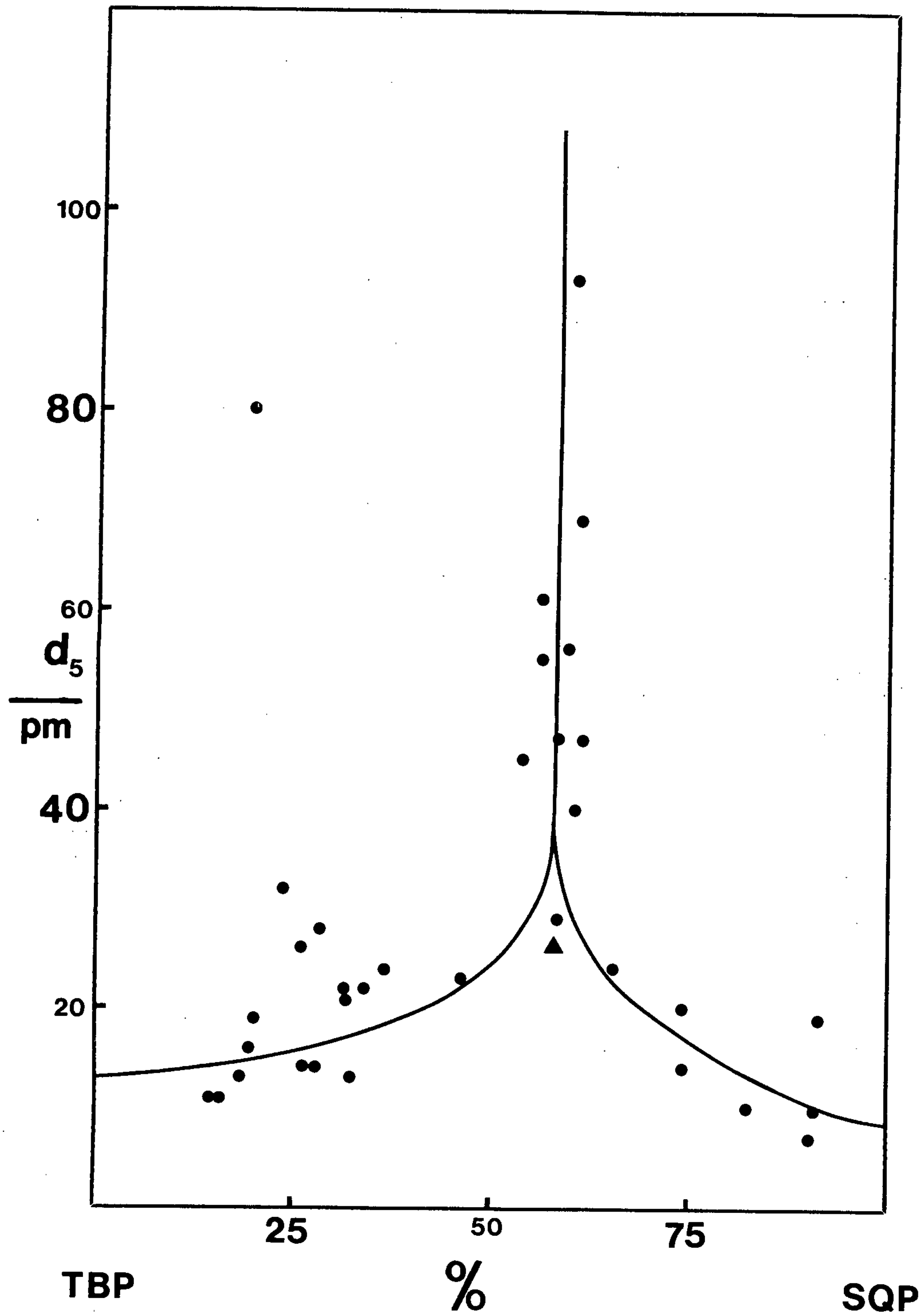

Figure 17. Plot of distortions (%) which arise as a function of the proximity (d_5) of the nucleophile to the zinc. The outlier (d_5 = 80 pm; 25%) is discussed in the text.

From Figure 17 we may classify the compounds into three broad types: (i) those intermediate between TBP and SQP, for which $d_5 > 30$ pm; (ii) those distorting towards SQP and (iii) those distorting towards TBP. Groups (i) and (iii) were considered together and examined as previously described by Bürgi[6] for five coordinate cadmium complexes.

(ii) Substitution Mechanism

Following Bürgi's approach, the compounds were treated as distorted TBP and we sought a correlation between the displacement z (Table 1) of the zinc ion from the equatorial plane defined by D_2, D_3 and D_4 and the proximity of the attacking nucleophile. Because there are large differences in atomic size of the various ligand atoms the compounds were grouped as (a) those containing at least two second row element atoms in the equatorial plane, and (b) those with two or more third row (or greater) elements as equatorial ligands. We note that, in general, the compounds of group (b) correspond to those of class (i), while those of group (a) are mostly represented in class (iii). This is not surprising, in view of the fact that the more bulky ligand donor atoms are more likely to be accommodated in a TBP conformation only, rather than in the sterically more crowded SQP.

We calculated the weighted average interatomic distances, $Zn - D_{equatorial}$, for the two groups as 199 pm and 235 pm respectively, and obtained correlations by plotting d_1 and d_5 against z, as is shown in Figures 18a and 18b. Following the method used by Bürgi in his analogous study of five coordinate cadmium complexes, we reflected the d_5 vs z plot across the line z = 0 (as

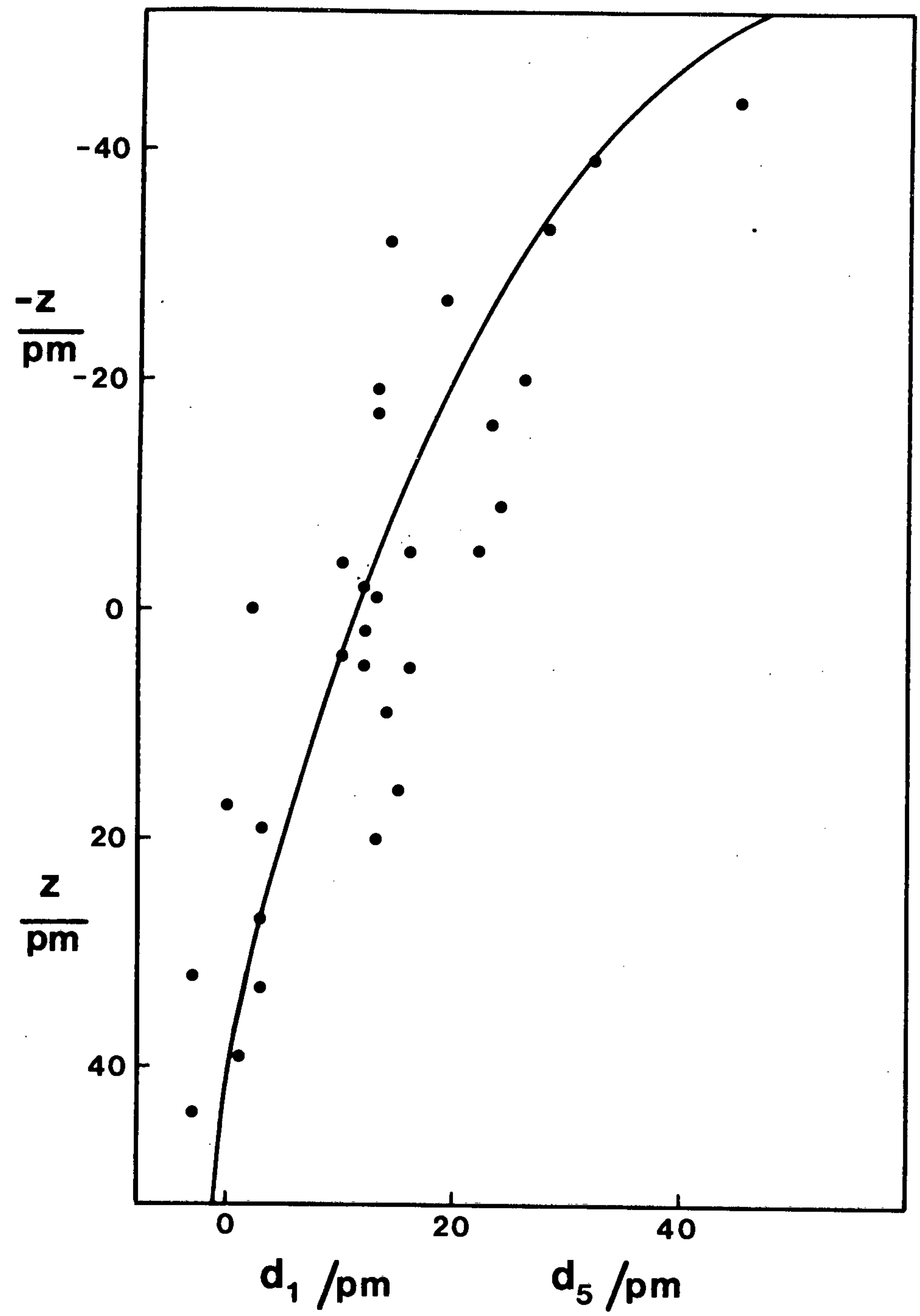

Figure 18a. Correlation between d_1, d_5 and z for compounds of group (a), obtained as shown in Figure 18b.

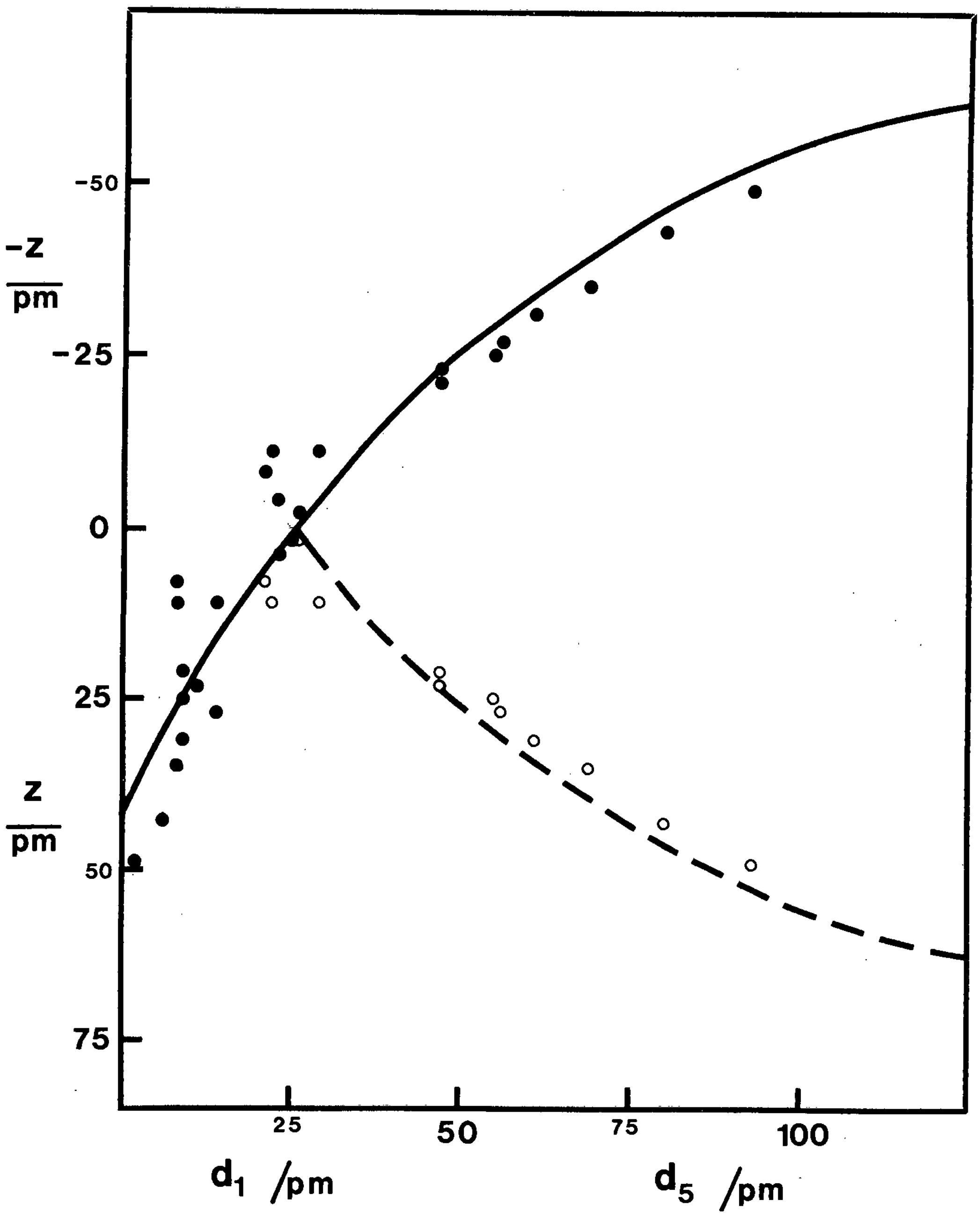

Figure 18b. Correlation between d_1, d_5 and z for compounds of group (b). Plot of d_5 *vs.* z (open circles and broken line) has been reflected across the line z = 0 to obtain a plot of d_5 *vs* - z.

shown in Figure 18b) in order to treat d_1 and d_5 as a single function of z so that $d_1 = f(z)$ and $d_5 = f(-z)$. The correlation figures show that as the nucleophile D_5 approaches the ZnL_4 tetrahedron at the fact opposite the leaving group D_1, the latter draws away from the zinc and the resulting ZnL_3 pyramid flattens. In the intermediate

$$[D_5 \; ... \; ZnL_3 \; ... \; D_1]$$

$z = 0$, d_1 and d_5 are equal and have values of 12 pm and 26 pm for groups (a) and (b) respectively. This intuitively expected lengthening of the axial bonds in the TBP intermediate or transition state has also been obtained in an *ab initio* calculation on the model system[34]

$$X^- + CH_3F \rightarrow XCH_3 + F^-$$

where the axial bond has been shown to be 30 pm in excess of the standard C-F bond length (148 pm).

The data sets were fitted to the logarithmic curve

$$d_1, d_5 = f(\pm z) = a \log(\pm z + z_{max}) + b$$

where z_{max} is the maximum out of plane displacement of the zinc atom from the plane $D_2D_3D_4$. This occurs when the attacking nucleophile D_5 is at an infinite distance from the ZnL_4 tetrahedron. The maximum displacements are calculated as 66 pm for group (a) and 79 pm for group (b).

Least-squares fit to the two data sets yielded the equations

$$\begin{array}{ll} \text{group (a)} & d_1, d_5 = 106 - 52 \log(\pm z + 66) \\ \text{group (b)} & d_1, d_5 = 294 - 141 \log(\pm z + 79) \end{array} \qquad \text{........ (1)}$$

These were transformed to:

$$\begin{aligned} &\text{group (a)} \qquad d_1,\ d_5 = -52\ \log\left\{{}^{(\pm z\ +\ 66)}/{}_{109}\right\} \\ &\text{group (b)} \qquad d_1,\ d_5 = -141\ \log\left\{{}^{(\pm z\ +\ 79)}/{}_{121}\right\} \end{aligned} \quad \ldots\ldots (2)$$

in order to make direct comparison with Pauling's formula $d = -C \log n$ which describes the variation of interatomic distance increments d with bond number n.

We thus obtain:

$$\begin{aligned} &\text{group (a)} \qquad n_1,\ n_5 = (\pm z + 66)/109 \\ &\text{group (b)} \qquad n_1,\ n_5 = (\pm z + 79)/121 \end{aligned} \quad \ldots\ldots\ldots\ldots\ldots (3)$$

$$\begin{aligned} &\text{group (a)} \qquad n_1 + n_5 = 1.2 \\ &\text{group (b)} \qquad n_1 + n_5 = 1.3 \end{aligned} \quad \ldots\ldots\ldots\ldots\ldots\ldots\ldots\ldots (4)$$

Therefore the bond numbers vary linearly with z and their sum is constant at approximately unity. This implies that, as substitution proceeds, the D_5 - Zn bond is created at the expense of the Zn - D_1 bond. The fact that $n_1 + n_5 > 1$ may indicate d-orbital contribution to axial bonding.

We failed to find any structural correlation for the square pyramidally distorted structures. We sought a sequential change of the displacement x of the zinc atom out of the basal plane $D_1D_2D_4D_5$ with d_5 (Table 1) but found no convincing relation. Possibly the SQP branch of the reaction coordinate mapped in Figure 17 represents a 'cul de sac' of the reaction pathway into which the compounds have been forced by intramolecular steric requirements or crystal packing forces or both.

The correlation between the axial distance increments d_1 and d_5 is shown in Figure 19 for the compounds of group (b). The data were fitted to Pauling's equation $d = -C \log n$ where C is an empirical constant. Holding the sum of the bond orders n_1 and n_5 to the values obtained in equation 4 we obtain the equation

$$10^{-d_1/C} + 10^{-d_5/C} = 1.2;\quad 1.3 \quad \ldots\ldots\ldots\ldots \quad (5)$$

which yields C values of 57 and 146 for groups (a) and (b) respectively.

This hyperboloid relation between the two distance increments mirrors that found in the linear triatomic systems examined by Bent[4] and shown in Figure 3. The corresponding data for the compounds of group (a) are far more widely scattered than those of group (b), shown in Figure 19. This greater scatter may result from the particular distortions which the groups respectively exhibit. Group (a), containing the smaller ligand atoms, is more capable of adopting a "distorted" TBP conformation than group (b), where a "purer" TBP predominates. This results in the Zn - D_1 and Zn - D_5 bonds lying in a straighter line for group (b) than they do for group (a), hence $D_1 \ldots\ldots Zn \ldots\ldots D_5$ approaches the linear, three centre, four electron system more closely for group (b) than it does for group (a).

In our model of the reaction,

$$D_5 + L_3ZnD_1 \rightarrow [D_5 \ldots\ldots ZnL_3 \ldots\ldots D_1] \rightarrow D_5ZnL_3 + D_1$$

the intermediate is assumed to be that structure for which $d_1 = d_5$. The values of C (from equation 5) were used to calculate d_1 and d_5 for $n_{1,5} = 0.6;\ 0.65$ yielding distance increments of 13 pm for group (a) and 27 pm for group (b). These values are in close agreement with those obtained by putting $z = 0$ in equation 1.

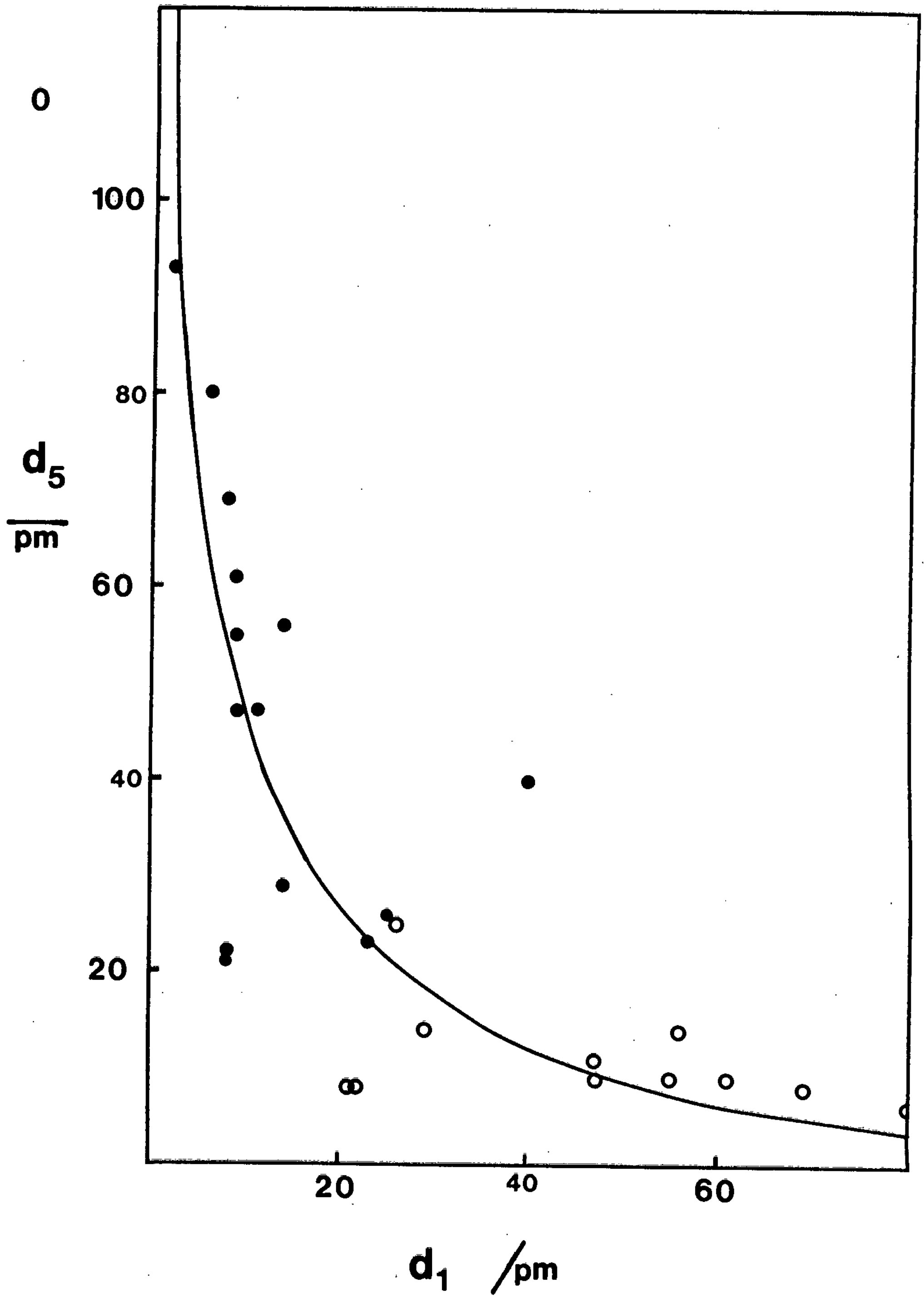

Figure 19. Correlation of d_1 and d_5 for compounds of group (b). Curve is drawn to equation 5.

The above discussion has focused on modelling the dynamics of the system. We have also considered the directional preferences of nucleophilic attack on the zinc ion. Figure 20 shows two possible approaches of the nucleophile to tetrahedral zinc. For an ideal "face" approach, F, the nucleophile-zinc-ligand angles are 180° for θ_{15} and 70.5° for θ_{52}, θ_{53} and θ_{54}; while an edge approach, E, gives rise to two pairs of angles of 125.3° and 54.7°.

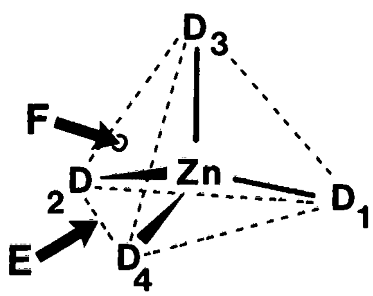

Figure 20. Diagram showing face (F) and edge (E) approach of the nucleophile to the ZnL_4 tetrahedron.

A scatter plot of the angles subtended between D_5 and the ZnL_4 tetrahedron is shown in Figure 21. This shows that the approach cannot be classified as either F or E, but as somewhere between. This is in agreement with the result obtained from Figure 17 which shows that the conformations at the early stage of reaction, ($d_5 > 30$ pm) are displaced approximately 57% towards SQP. Examination of Appendix 1 shows that, on average, the nucleophilic attack is inclined away from D_3 ($\theta_{53} = 92.9^{\circ}$, $\theta_{52} = 83.6^{\circ}$, $\theta_{54} = 81.7^{\circ}$). We note that D_3 acts as pivot for the Berry pseudorotation but this could be simply due to the nomenclature we employed.

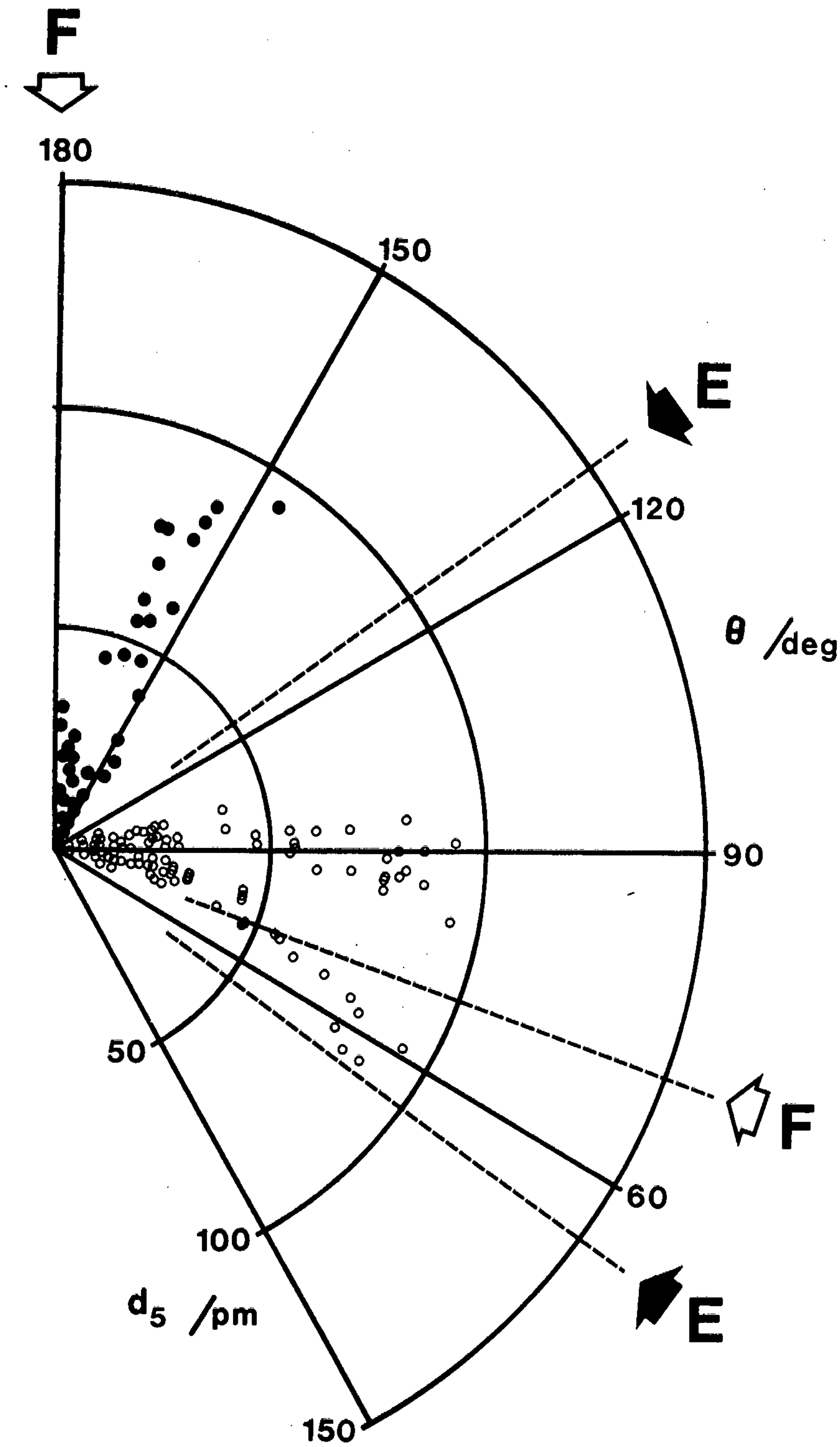

Figure 21. Scatter plot of d_5 *vs.* θ_{15} (full circles) and d_5 *vs.* θ_{5i} (i = 2, 3, 4) (empty circles).

SUBSTITUTION REACTIONS AT NICKEL

In the above analysis of the five coordinate ZnL_5 fragments, as in the investigations of pentavalent cadmium[6] and tin compounds[8], the effect of the d-orbital electron configuration on the geometry could be ignored due to completely filled d-sublevels. It has been shown however, that unfilled d-electron configuration may well have a marked effect on conformation[35,36]. Thus for low-spin d^8 TBP conformations it has been predicted that the axial bonds will be stronger, and hence shorter, than the equatorial ones, while in the corresponding SQP the apical bond is expected to be weaker and longer than the basal ones. In the case of high-spin d^8 these rules are expected to be somewhat relaxed. For the TBP a d^9 configuration has no effect on the bond lengths, while d^7 yields a slightly stronger axial bond. Both d^7 and d^9 show slightly stronger apical bonds in the SQP, than the low-spin d^8 configuration. Table 2 lists the spin states (as far as they have been reported) and the charges on the nickel atom.

In the series of nickel compounds, as in that of zinc, there is a smooth progression of conformations from TBP to SQP, mimicking the Berry pseudorotation coordinate. If the compounds are viewed as distorted TBP, then d_1 and d_5 are representative of the axial bonds, while if they are viewed as distorted SQP, d_3 represents the apical bond. This is represented in Figure 11. In order to examine the dependence of the axial bond (TBP) and the apical bond (SQP) on the degree of distortion, we plotted d_5 and d_3 against percentage distortion from ideal TBP to ideal SQP in Figures 22(a) and 22(b) respectively.

<u>Footnote</u>: We use the term <u>axial</u> when referring to TBP conformation, as opposed to <u>apical</u>, which we use when referring to SQP.

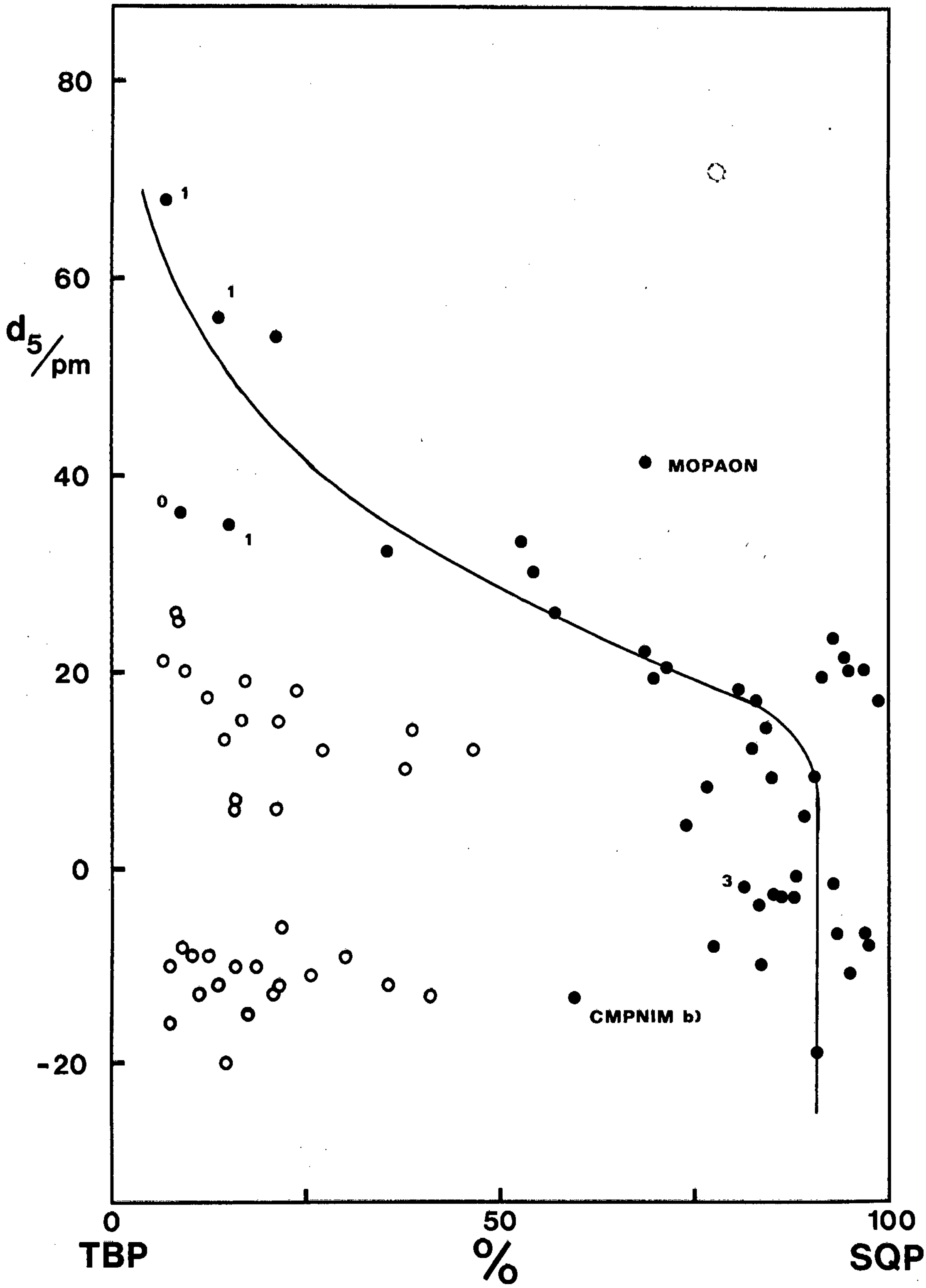

Figure 22a. Axial (d_5) and apical (d_3) distance increments vs. percentage distortion from TBP → SQP. Full circles correspond to structures considered to lie on the addition pathway.

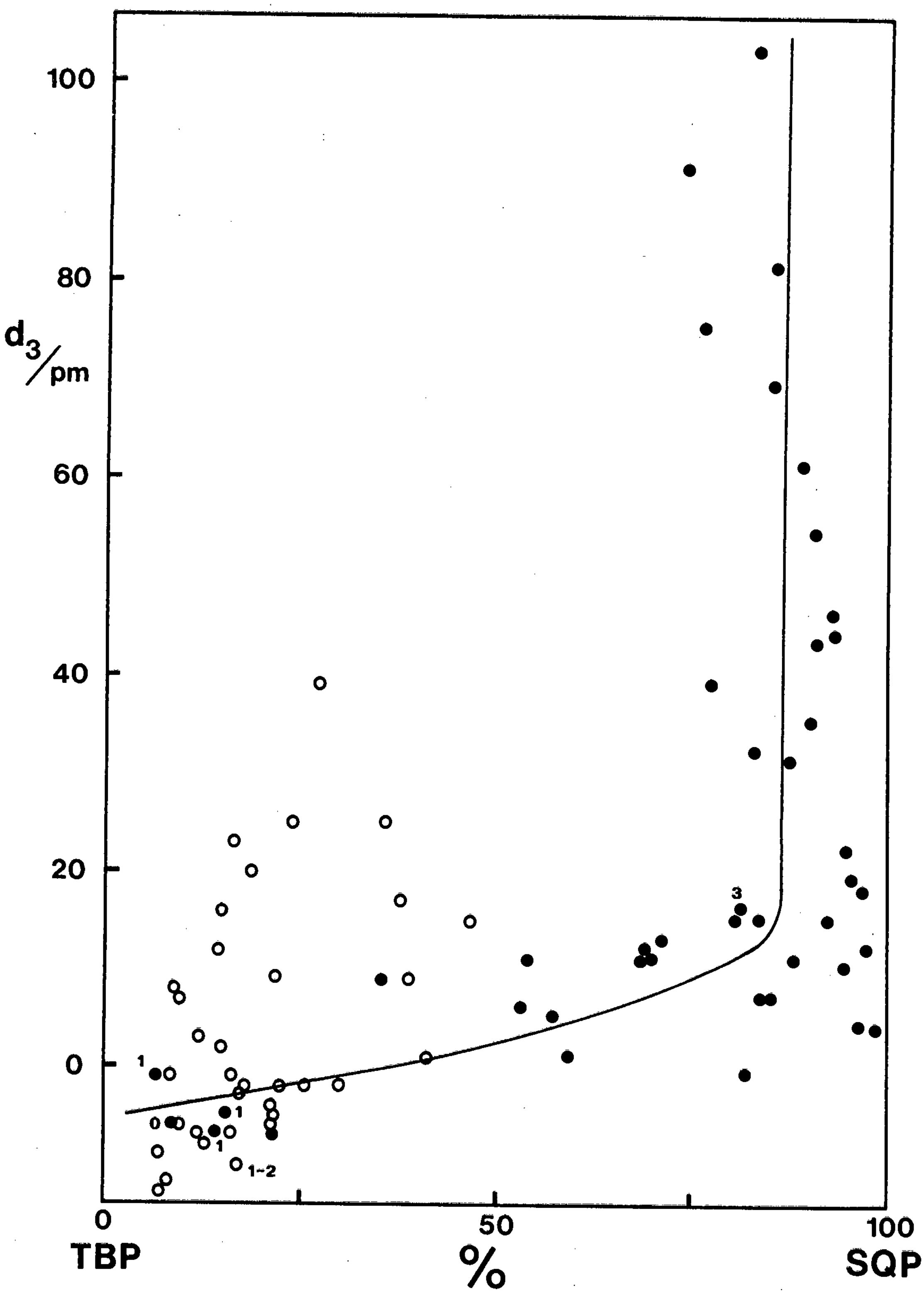

Figure 22b. Empty circles correspond to compound distorted away from the pathway. Numbers next to points refer to the charge on the Ni atom. Compound CMPNIM (b) and MOPAON are accounted for in the text.

From Table 2 and Figure 22 the following conclusions may be drawn: (i) axial d_1 and d_5 are generally smaller for low spin d^8, (ii) d_1 and d_5 are shorter for d^8 than for d^9, (iii) in one case of a d^7 compound d_1 and d_5 are shorter than for the d^9 complexes and (iv) d_3 is in general quite long for low spin d^8 complexes, but shorter for d^9. All of these conclusions are in line with the predicted pattern.

Figure 22(a) hints at a reaction pathway in that the compounds represented by filled circles may be visualised as lying along some distortion coordinate, while the open circles do not. Figure 22(b) supports this hypothesis, since the filled circles may again be seen to lie on a reaction pathway, while the empty circles are once again scattered. That the points for compounds MOPAON and CMPNIM(b) lie somewhat off the coordinate drawn might be due to considerable strain within the molecules. MOPAON, whose structural formula is shown in Figure 10, contains 2 six-membered rings, well recognised as being sterically hindering for five coordinate compounds. CMPNIM contains the large and bulky benzophosphole ligand, which may be expected to have some effect on the conformation. CMPNIM exists as two allogon isomers, the (a) form lying well off the coordinate of Figure 22, the (b) form closer to it. The fact that it is the square pyramidal form of the compound which lies closer to the coordinate, lends credence to the following assumption.

The adherence of the compounds to the coordinate dependent on d_3, i.e. on the proximity of the apical ligand in a SQP, is in agreement with the suggestion[24] that association reactions at square planar nickel centres proceed via a SQP intermediate. We thus identify 2 groups of pentavalent nickel compounds: (i) those whose distortions mirror the pattern expected in an association reaction between a square planar NiL_4 moiety and an attacking nucleophile (D_3) leading to a SQP intermediate (full circles in Figure 22, compounds 1-43 in Table 2) and (ii) those which due to some combination of inter- and intramolecular restrictions are forced off this reaction coordinate (empty circles in Figure 22, compounds 44-78 in Table 2).

(i) Association

The association reaction leading from a square planar, four-coordinate complex to a square pyramidal one can best be represented by a correlation between the proximity of the attacking nucleophile (d_3) and the degree of pyramidality of the SQP (x). Figure 23 shows that as the nucleophile D_3 approaches the nickel centre from infinity, so the displacement of Ni out of the basal plane increases from zero, until it reaches 44 pm in the case where d_3 = 0 pm. The data have been fitted to an exponential curve such that

$$x = 44.2\ e^{-0.02\ d_3} \quad \ldots\ldots\ldots\ldots (6)$$

whence $$d_3 = 115.2 \log (x/44.2) \quad \ldots\ldots\ldots\ldots (7)$$

Equation 7 is again reminiscent of Pauling's formula[7] implying that a geometrical measure for bond number n is x/44.2. Although all the data in Figure 23 were used in calculating the least squares line, it appears that for d_3 < 10 pm the relation between the two parameters changes, in that some of the points lie well above the line at values of x ≈ 55-60 pm. Indeed, an investigation of those compounds (Nos. 44-78) which do not fall on the coordinates shown in Figure 22, and hence are not believed to map the association reaction, shows that in the majority of cases the x values lie in that range, i.e. appear to be constant. Moreover from Figure 23 it seems that for $d_3 < 10$ pm the compounds distort from almost pure SQP to TBP. Thus the approach of the nucleophile (D_3) towards the NiL_4 moeity seems to be accompanied by increasing pyramidalisation at the nickel, leading to a square pyramidal intermediate, which then distorts, presumably via the Berry mechanism, towards a TBP when $D_3 < 10$ pm. ESPNIQ, TEDTEP and CAPPNC, whose structural formulae are shown in Figure 10, contain sterically hindering 4- and 6-membered rings, hence explaining their scatter from the line.

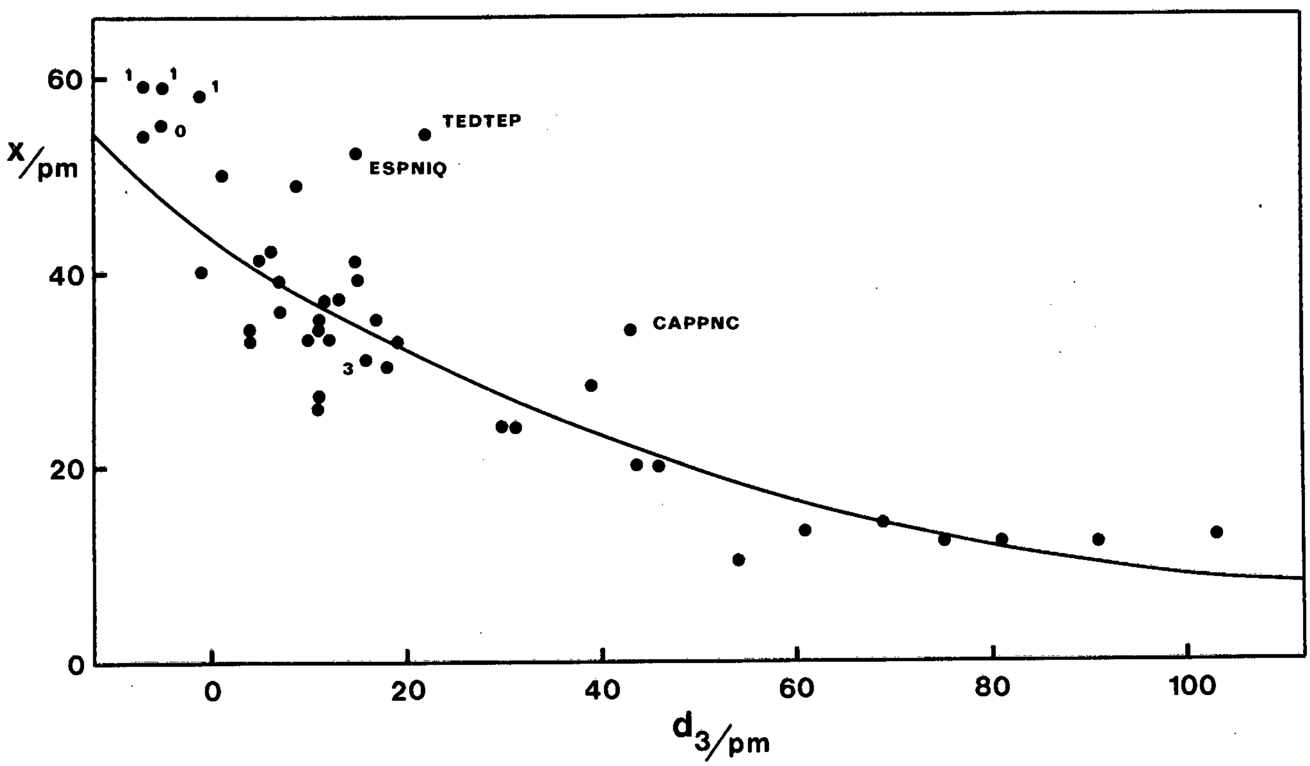

Figure 23. Dependence of out-of-plane displacement x on d_3. Numbers next to points indicate the charge on nickel. Scatter is discussed in the text. Curve drawn to equation 6.

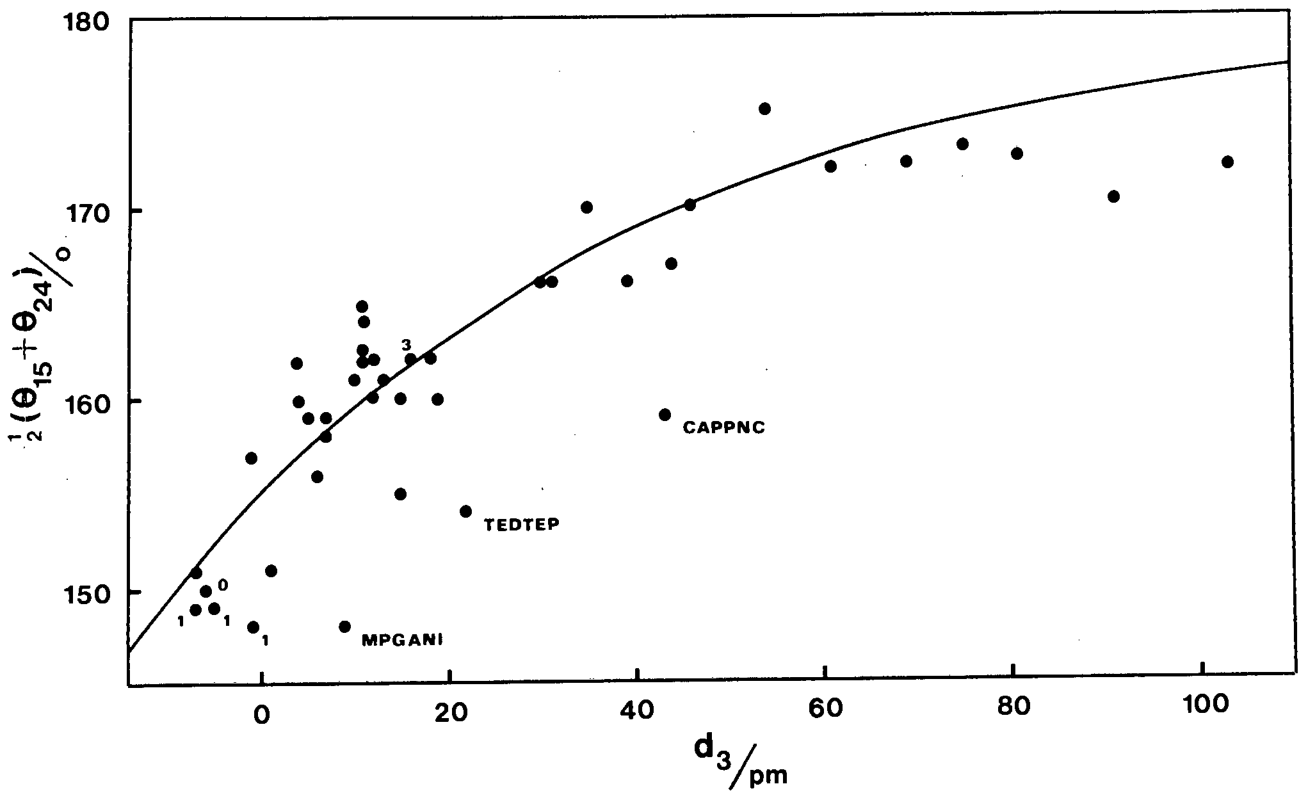

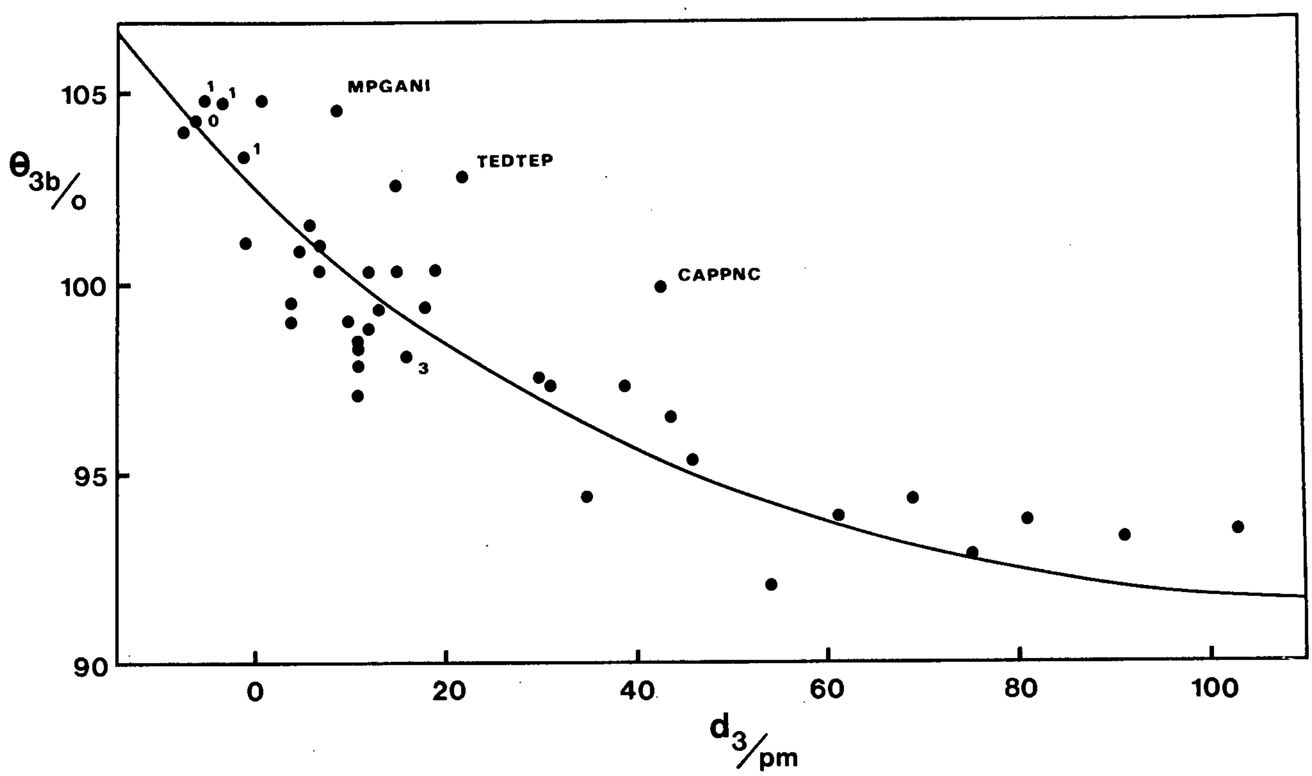

<u>Figure 24</u>. a) Plot of the average trans-basal angle *vs.* d_3,
b) Plot of the average apical basal angle *vs.* d_3.
Numbers next to points indicate the charge on nickel. Scatter is discussed in text.

There has been much discussion concerning the value of the trans-basal angle (θ_{15} and θ_{24}) in an ideal SQP, although it is generally agreed that this will depend on d-electron configuration[35,36,37]. Even so Muetterties and Guggenberger[14] set the value of this angle at 156^{o} in their study of pentavalent compounds of both main group- and transition elements. Other values have been 160^{o}, 150^{o} and 152^{o}, all for compounds with filled d-sublevels[15,38], and 164^{o} for d^{8} species[35]. Figure 24 shows plots of the average trans-basal angle $((\theta_{15} + \theta_{24})/2)$ and the average apical-basal angle (θ_{3b}) against the proximity of the incoming nucleophile D_3. The data have been fitted to a line calculated from equation 6, assuming a bond length of 205 pm between Ni and D_1, D_2, D_4 and D_5, a value well within the range found for the compounds. The curves show that the average trans-basal angle changes from 180^{o} to 155^{o} as d_3 tends to zero, thus reflecting the behaviour of the square planar NiL_4 as D_3 approaches this moeity. Structural formulae, shown in Figure 10, for MPGANI and MAZNIP shown why these compounds are distorted from the coordinate shown in Figure 24.

In order to examine in more detail the distortions which the NiL_4 fragment undergoes, we calculate an additional parameter ϕ (listed in Appendix 1), defined as the average angle between the normals to the pairs of planes D_1NiD_2, D_4NiD_5 and D_1NiD_4, D_2NiD_5. Figure 25 defines ϕ and shows how ϕ and the trans-basal angles vary along the pathway we have proposed. Figure 26 shows a plot of ϕ against θ_{15} and θ_{24}. The solid line represents the reaction coordinate for the scheme outlined in Figure 25. The branched part of the reaction coordinate shown in Figure 26, is of course the Berry coordinate, corresponding to the rotation of the SQP into a TBP.

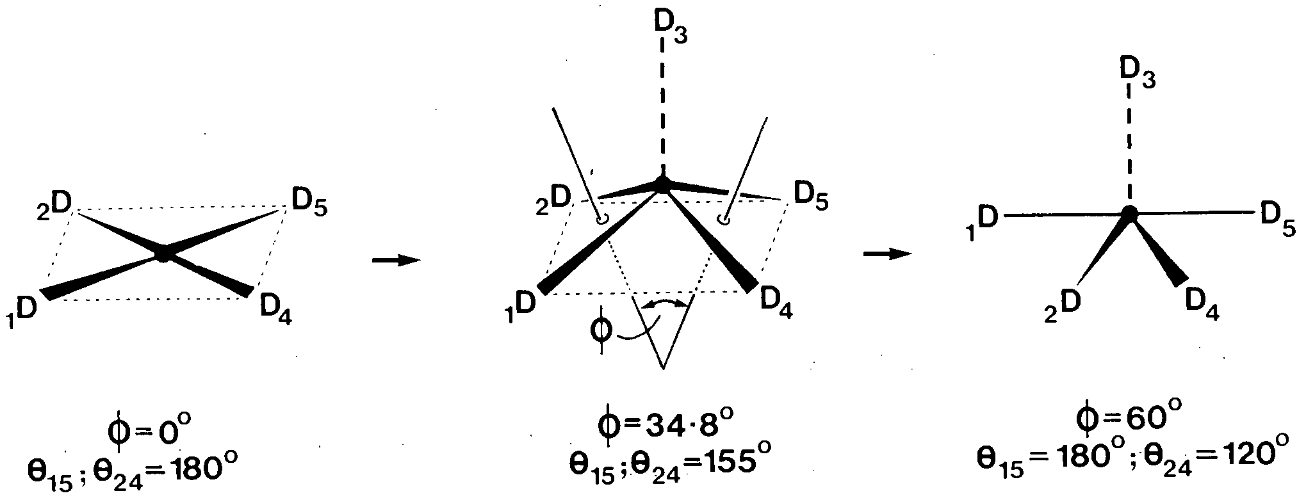

Figure 25. Definition of ϕ and diagram showing how ϕ, θ_{15} and θ_{24} vary along the proposed reaction pathway.

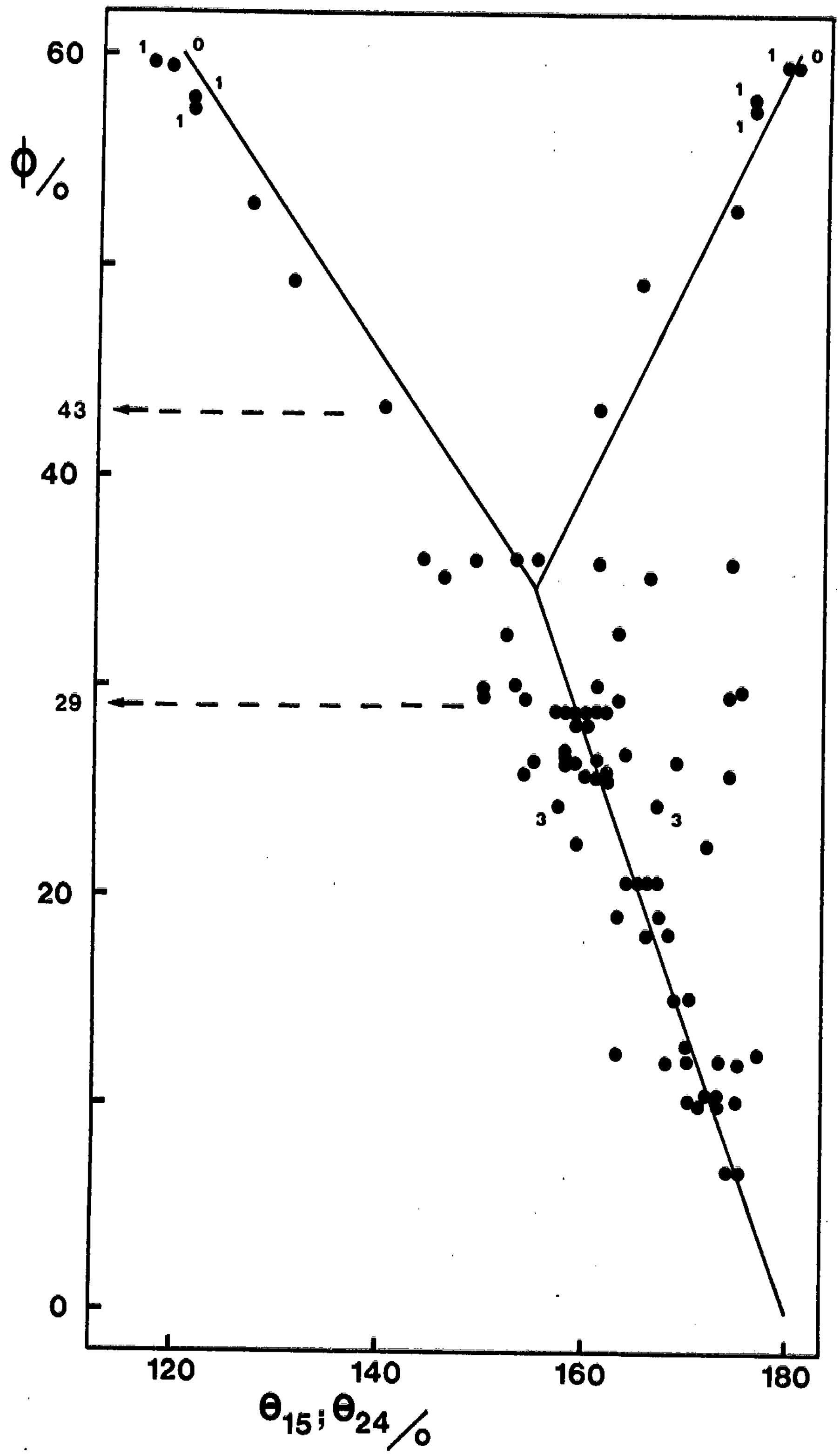

Figure 26. Plot of ϕ against θ_{15} and θ_{24}. Solid line corresponds to reaction coordinate outlined in fig. 6. Numbers next to points refer to charge on nickel.

(ii) Pseudorotation

We employ the same method in mapping the Berry coordinate as used earlier for the zinc compounds, and Figure 27 shows a plot of $217.9 - \sum_{ij} |\delta_{ij}(C) - \delta_{ij}(SQP)|$ against $\sum_{ij} |\delta_{ij}(C) - \delta_{ij}(TBP)|$.

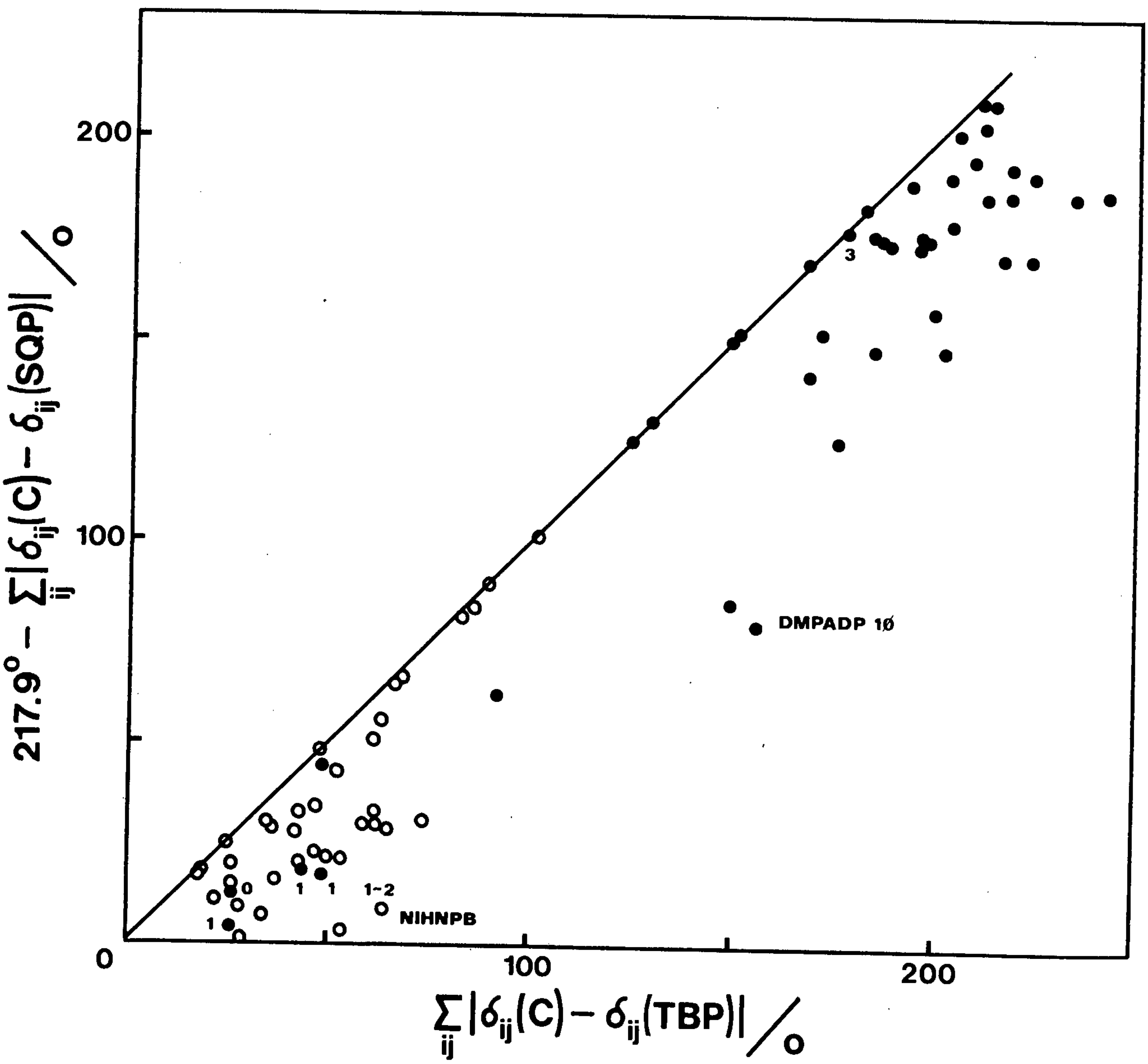

Figure 27. Diagram showing adherence of the compounds to the Berry coordinate shown as the straight line. Full circles correspond to compounds mapping the association reaction. Numbers refer to the charge on the nickel.

There is considerable scatter from the minimum energy coordinate, but it is significant that those compounds not considered to map the association reaction (empty circles) exhibit less scatter than those that do (full circles). As earlier, we surmise that the distortions of the compounds away from the Berry coordinate are brought about by structural restrictions imposed by a combination of steric- and electronic requirements of the ligands, and that these are more evident in the compounds which map the association reaction. In terms of our interpretation, we may quote Bürgi[40] "the behaviour of the SQP complexes becomes visible already in the way the TBP deforms", thus explaining why these SQPs distort away from the coordinate. NIHNPB is a hydride of the type MHL_4, which is pseudotetrahedral, and has long been known not to pseudorotate[39]. DMPADP 10 contains a four membered ring, as well as the large and bulky 2,9-methyl-1,10-phenanthroline ligand, thus possibly explaining its distortion. Structural formulae are shown in Figure 10.

(iii) Dissociation

Theoretical consideration have rather vaguely implied equatorial dissociation of a TBP intermediate[23], or apical dissociation of a SQP intermediate[24], in substitution and isomerisation reactions respectively, with experimental evidence seeming to support the latter. However in at least four cases[41-44] departure of an axial ligand in a TBP has been indicated. We apply a method outlined by Dartiguenave *et al*[41] to map the geometrical reaction coordinate for the gradual removal of an axial ligand in a TBP along the C_3 axis, ie., the transition from a trigonal bipyramid with C_{3v} symmetry to a monocapped tetrahedron. This method involves calculating the normalised shift parameter $s = (\bar{d}_{eq} - 3z)/\bar{d}_{eq}$ and correlating it with the sum of the angles at the central metal atom along ($\Sigma\theta_{1e}$) and around ($\Sigma\theta_{ee}$) the threefold axis respectively. $\bar{d}_{eq}$ is the averaged metal to equatorial ligand distance, $\Sigma\theta_{1e} = \theta_{12} + \theta_{13} + \theta_{14}$ and $\Sigma\theta_{ee} = \theta_{23} + \theta_{34} + \theta_{24}$. This method was originally introduced in support of a suggestion that the compound BAPKEI, whose structural formula is shown in Figure 10, lies along the reaction pathway for homolytic Ni---CH_3 bond cleavage leading to a tetrahedral Ni(I) species.

Figure 28 shows a plot of $\Sigma\theta_{1e}$ and $\Sigma\theta_{ee}$ versus s for those compounds not considered to map the association reaction (empty circles), as well as for the more trigonal bipyramidal conformations of the second group (full circles). The solid line indicates the calculated coordinate, and it seems as if both groups adhere to it equally well. The fact that it is the Ni(I) species which are in general furthest removed from the C_{3v} toward the T_d conformation supports firstly the suggestion originally made[41], and secondly the assumption that there may be an element of axial departure in a TBP intermediate.

Since we are mapping essentially a substitution reaction which occurs via an associative step, it is of interest to correlate the approach of the nucleophile with the departure of the leaving group. In the analysis of the molecular geometries we assigned ligand D_1 the better leaving group qualities, while in the derivation of Figure 28 we assumed D_5 to be the leaving group. Figure 29 shows the correlation between d_3, d_1 and d_5,

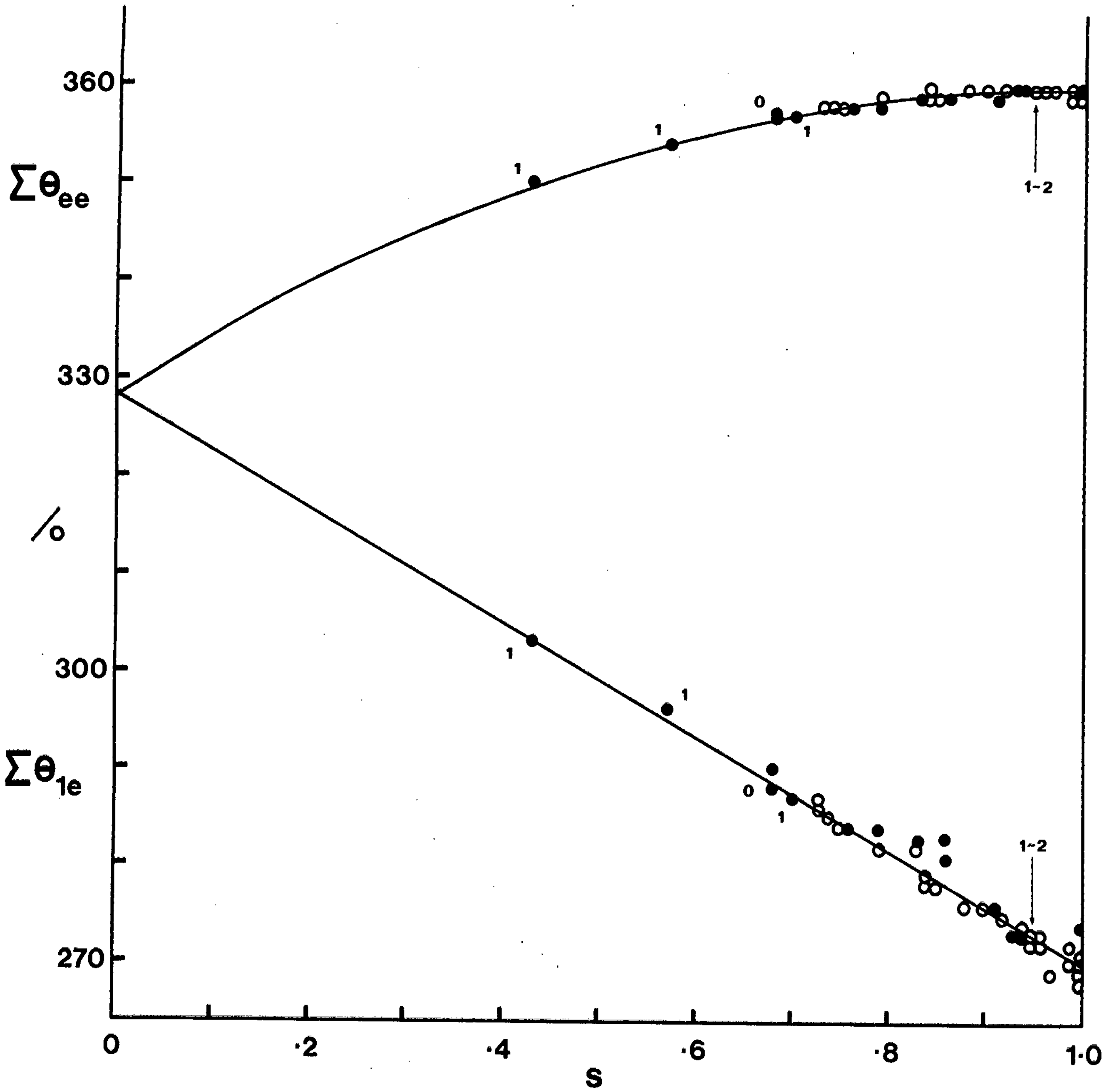

Figure 28. Diagram showing $C_{3v} \rightarrow T_d$ transition for compounds which map the association reaction (full circles), and those that do not (empty circles). $\Sigma\theta_{ee}$, $\Sigma\theta_{1e}$ and s are defined in the text. Numbers next to points refer to the charge on nickel. Calculated reaction coordinate is shown by the solid line.

and although scattered, the plots do show a trend. It appears that the approach of D_3 to the NiL_4 fragment is accompanied at first by very little, if any, lengthening of the axial bonds. However, small decreases of d_3 below ca. 20 pm seem to bring about large increases in d_1, and d_5. This trend suggests that the formation of the SQP intermediate precedes any departure of a leaving group, which may occur once the SQP→TBP transition has taken place, thus allowing the nucleophile to bond more closely to nickel.

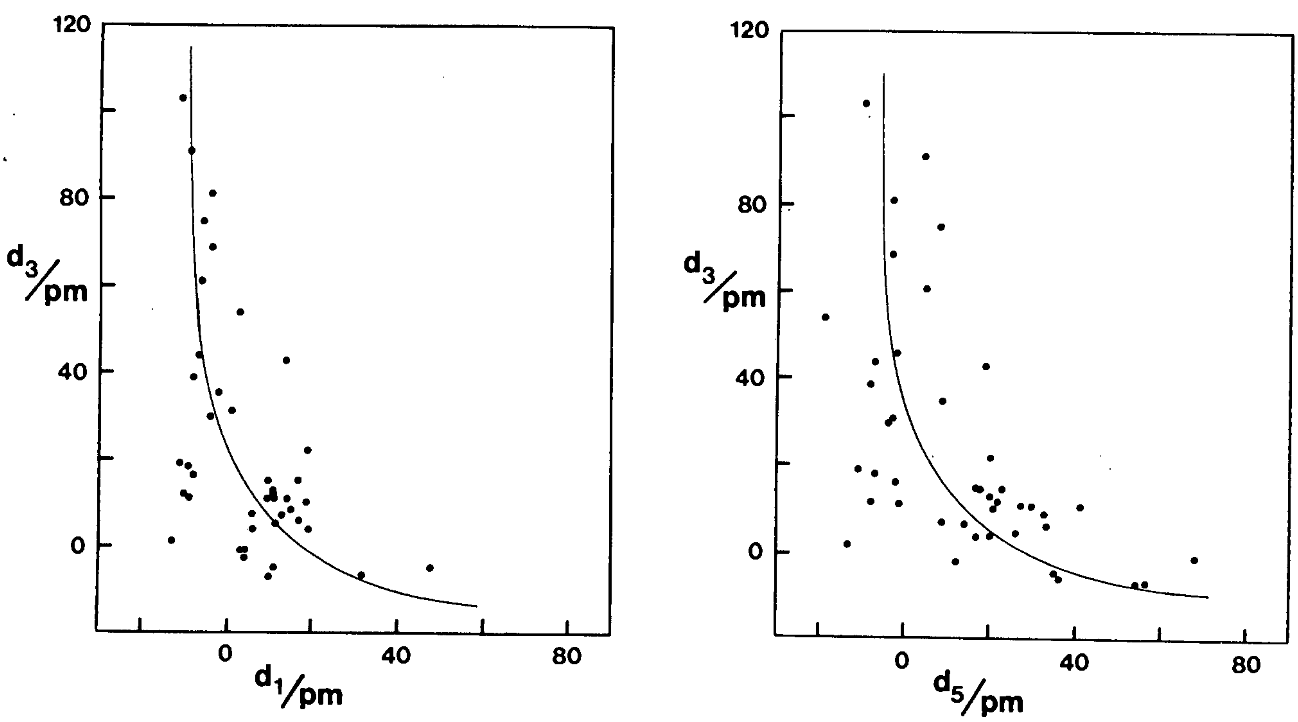

Figure 29. Correlation of (a) d_3 with d_1 and (b) d_3 with d_5, for compounds mapping the reaction pathway.

DISCUSSION AND EXPERIMENTAL OBSERVATIONS

The correlations presented here are consistent with the sequence of reversible steps outlined in Figure 30. Thus tetrahedral zinc complexes undergo a typical S_N2 reaction proceeding via a five coordinate intermediate or transition state (step `C´), which initially is TBP. This pentavalent moeity may pseudorotate into a SQP conformation (step `B´), which in terms of the substitution reaction is a "cul de sac", in that dissociation occurs from the axial positions of a TBP (step `C´ again). Obviously pseudorotation may continue beyond the SQP stage to yield a new TBP conformation. The suggestion that the formation of the Zn---D_5 bond involves the same type of charge separation as the cleavage of the Zn---D_1 bond, ie., that the two processes (and thus their coordinates) are mirror images of each other, has received support from a recent study. An *ab initio* investigation of the reaction

$$X^- + CH_3X \rightarrow XCH_3 + X^-$$

has suggested the formation of a symmetrical transition state which has been supported by experimental evidence[45].

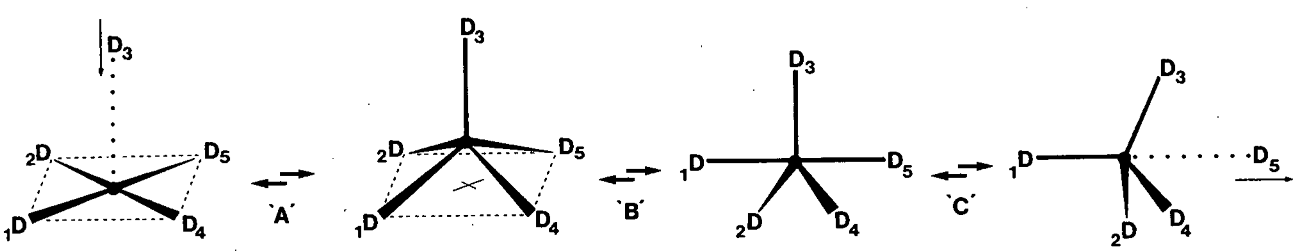

Figure 30. Reaction sequence corresponding to reversible association at a square planar centre (`A´), reversible pseudorotation of the SQP into a TBP (`B´) and reversible axial dissociation of the TBP (`C´).

However, whereas bond formation and cleavage seem to occur simultaneously for the reaction at zinc, they seem to take place in two quite distinct steps at nickel. Dissociation may occur either via the reverse of the association reaction at square-planar nickel (step `A´), ie., from the apical position of a SQP, or from the axial position of a TBP (step `C´), formed by pseudorotation of the initial SQP (step `B´).

ZINC

Five coordinate intermediates have been proposed for a number of substitution and isomerisation reactions of tetrahedral zinc complexes. Thus, for the reaction of bis(N,N-di-μ-butyldithiocarbamato)zinc(II) with iodine in cyclohexane, the penta-coordinate intermediate, shown in Figure 31 has been proposed[46]. Bis(*o*-ethylxanthato)pyridine zinc(II), which has been used in this study (EXAPYZ)[47], has been proposed as lying along the reaction coordinate of the reaction

$$Zn(exa)_2 + L \rightleftarrows Zn(exa)_2L \qquad (4)$$

exa = *o*-ethylxanthato, L = py, EtOH, $(CH_3)_2CO$,DMSO

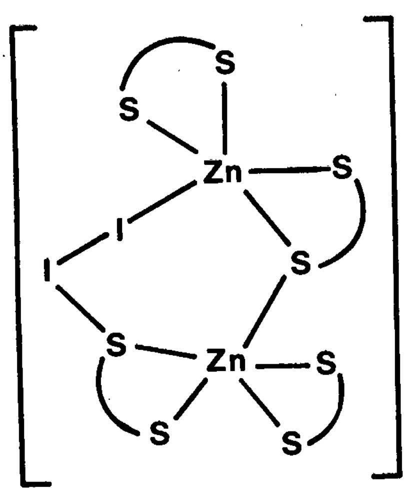

Figure 31. Proposed intermediate From ref. 46.

The labile nature of zinc thiourea complexes in solution has been examined[48] and the ligand exchange has been found to occur via an associative mechanism. Such a bimolecular ligand exchange mechanism has also been proposed for thiocumato zinc(II) derivatives[49]. One of the proposals advanced to explain the acetate scrambling process in the meso-(2,3-butylenediamine) tetraacetic acid complex with zinc(II) involves a penta-coordinate intermediate of either TBP or SQP conformation[50]. The addition of sulphur to dithiobenzoato complexes of zinc(II) has been studied, with the conclusion that the mechanism of the reaction involves addition of a sulphur atom and a subsequent rearrangement of the ligands about the zinc[51].

Penta-coordinated intermediates have also been proposed for a number of bio-chemical reactions. In the enzyme catalysed reversible hydration of carbon dioxide by carbonic anhydrase, the intermediate shown in Figure 32 has been suggested[52,53]. A penta-coordinate intermediate has also been proposed in the catalytic cycle involving alcohol dehydrogenase and nicotinamide coenzyme[54], while a general examination of the active site geometries of zinc enzymes has been undertaken[55]. In all cases the metal ion is bonded by three protein ligands and water in a distorted tetrahedral arrangement, and it is suggested that the substrate may bind at a fifth coordination site.

Interestingly, there is also a report of a fluxional penta-coordinate zinc complex[56]. A ^{13}C n.m.r. investigation has been carried out on the complex $[ZnXL]^+$ in nitromethane (X = halide, NCS^- or ClO_4^-; L is a quadridentate methyl-substituted tetraazacyclotetradecane ligand). A dynamic process which possibly involves the interconversion of axial and equatorial N-methyls, via a Berry mechanism, is indicated as shown in Figure 33. This complex was used in our study, compound CTAZZN.

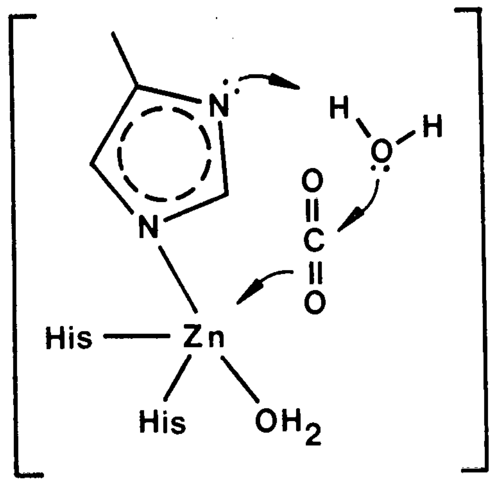

Figure 32. Intermediate proposed for hydration of CO_2 by carbonic anhydrase. From ref. 52.

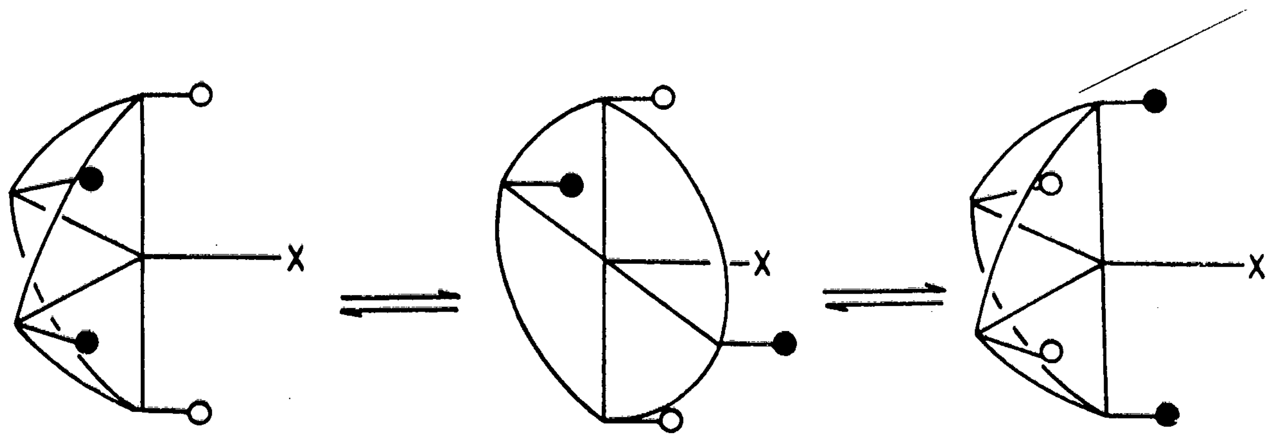

Figure 33. Berry pseudorotation of compound CTAZZN. From ref. 56.

NICKEL

Associative steps, in some cases rate-determining, leading to five-coordinate intermediates have been suggested for a number of substitution and addition reactions at square-planar nickel. Thus, for example, substitution of the ligands in square-planar dithiocarbamate and dithiophosphate complexes, by ethylenediamine and cyanide ion, has been rationalised in those terms[57], as well as the substitution of X^- by various nucleophiles in complexes of the type *trans*-[Ni(PEt_3)$_2$(o-tolyl)X] where X = Cl, Br, I, N_3, NO_2[58]. A pre-equilibrium involving a five-coordinate species has been indicated for ligand substitution reactions in bis(N-R-salicylaldiminato)nickel(II) complexes[59]. The rate of addition of 1,10-phenanthroline to bis(monothioacetylacetonato)- and bis(dithiophosphato)nickel(II) complexes is dependent on the rate of formation of a pentavalent intermediate[60], as is the addition of L to $[HNiL_3]^+$ where L = $P(Et)_3$[61]. The concept of such an intermediate is not limited only to addition and substitution reactions, but it has also been invoked in a mechanistic interpretation of intermolecular ligand exchange in a series of complexes *trans*-[$NiRXL_2$][62], and in the study of the interchange between coordinated and uncoordinated acetyl groups in 3,3^1-Ethylenebis(nitrilomethylidyne)di-2,4-pentanedionato(-2) nickel[63].

Fluxional behaviour of five coordinate nickel species is well established *in vitro* and has been proposed to occur *in vivo* as well, in that it has been suggested[64] that the nickel complex with human serum albumin is five-coordinate and in slow exchange. Complexes of the type ML_5 (L = phospite, PMe_3) have been studied[65,66] and shown to undergo intramolecular ligand exchange, presumably *via* the Berry mechanism. Similarily an investigation of the C_{2v} complexes $[NiX(PMe_3)_4]^+$ (X = Cl, Br, I), the bromide of which was used in this study (compound BMPNIB 1Ø - structural formula in Figure 10), revealed a "double Berry mechanism" with one of the equatorial phosphines acting as the pivot[67]. A fluxional five coordinate intermediate has also been suggested[68] for the carbonylation reaction of halo(bisligand)-organonickel(II) complexes.

In a series of papers[42,43,67,68,69] the results of studies on the dissociation of complexes of the type $[ML_5]^{2+}$, $[ML_4X]^+$ and $[ML_3X_2]$ where X = Cl, Br, I, CN and L = tertiary phosphine or phosphite are presented. In the case of $[ML_3(CN)_2]$ and $[ML_4X]^+$ apical departure of L from a SQP intermediate takes place, corresponding to step `A´of the reaction sequence in Figure 30. However in $[ML_5]^{2+}$ and $[ML_3X_2]^+$, where X is a halide, L leaves from the axial position of a trigonal bipyramid, corresponding to step `C´. Dissociation of a SQP complex is also indicated in the reaction of $[Ni(diars)_2Br]^+$ with CN^- (diars = *o*-phenylene-bisdimethylarsine)[70] and for the intermediate in the octahedral$\rightleftarrows$ square-planar interconversion of $[Ni(bbh)L_2]$ (L = pyridine; bbh = biacetyl bis-α-hydroxy benzylidenehydrazone(2-))[71].

English, Meakin and Jesson, in their detailed study of ligand association reactions at square-planar nickel[61], come to the same conclusion regarding the mechanism of that reaction as is presented in this work. Finally we would like to mention a study of the compound identified by the CCDC acronym INOPNI[72], a perspective view of which is presented in Figure 34. On the basis of the electronic spectra, neither a square-planar nor a five-coordinate conformation could be unambiguously assigned. Indeed the crystal structure of the compound reflected this, in that it revealed an extremely long bond in the apical position of an almost flat square pyramid.

It is remarkable to what extent the behaviour of the [ML_5] (M = Ni, Zn) fragment in crystals mirrors its generally accepted mode of behaviour in solution.

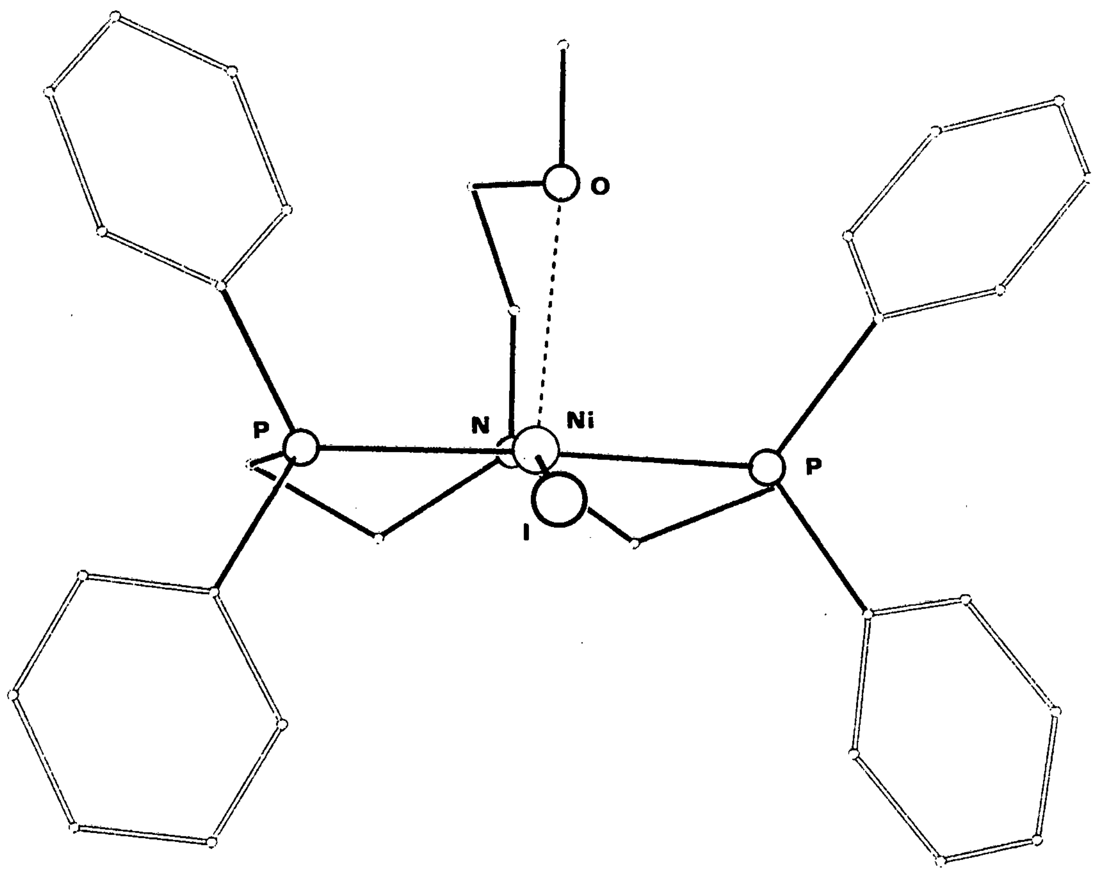

Figure 34. View of INOPNI showing the almost planar base of the SQP, with O in the apical position.

A CONCLUDING REMARK

We have examined a wide variety of crystal and molecular structures, with the only similarity amongst them being the central ML_5 moeity, the metal atom surrounded by its five ligand donour atoms. From this we have found correlations between certain parameters describing the geometry of that fragment throughout the various environments. These correlations, running like a thread through all the different molecular structures, must be brought about by the only factor common to all of them, the ML_5 unit. Of that there can surely be no doubt. In other words, the topographical features of the potential energy hypersurface for the ML_5 sub-system, in the solid state at least, are seen to be more-or-less independent of its various environments and of M and L. This insensitivity of the Born-Oppenheimer surface to the nature of the metal and ligand atoms was pointed out earlier in the study of the dissociation of YMX_3 and MX_4 tetrahedra[12]. In fact, this insensitivity has been implicitly demonstrated in all cases where reaction coordinates have been mapped from widely different molecular structures.

What might be queried, however, is the assumption that the features of the energy surface will not be altered much, even when the molecular environment of the fragment is composed of solvent molecules. In answer to this we point out that the reaction coordinates which we and others have mapped, have not only been proposed from theoretical considerations, but have also received much experimental support. Although this method of mapping reaction pathways is still quite new, it does seem as if "the proof is in the pudding". After all, is not the hypothesis underlying our approach tacitly accepted or supported by every study in which the behaviour of a molecular compound in solution is compared to, or justified by its solid state structure?

APPENDIX

The appendix contains the following tables:

A1 - interatomic angles (θ) for zinc compounds,

A2 - dihedral angles (δ) for zinc compounds,

A3 - interatomic angles (θ) for nickel compounds,

A4 - dihedral angles (δ) for nickel compounds,

A5 - dihedral angles (ϕ) for nickel compounds.

Table A1. Interatomic angles/° found in the zinc complexes.

No.	θ_{23}	θ_{24}	θ_{34}	θ_{12}	θ_{13}	θ_{14}	θ_{52}	θ_{53}	θ_{54}	θ_{15}
1	116	134	110	92	83	92	88	100	86	177
2	123	125	112	89	89	100	81	102	82	168
3	113	119	113	103	102	98	79	80	79	176
4	112	134	114	76	101	98	75	98	95	150
5	115	124	114	95	106	96	82	84	78	170
6	118	130	112	87	91	94	91	89	88	178
7	118	118	118	97	97	97	83	83	83	180
8	115	134	108	79	105	106	89	95	71	160
9	104	136	117	106	110	75	69	94	92	155
10	123	121	116	95	99	80	80	95	91	166
11	124	122	113	88	98	88	90	89	87	173
12	106	137	111	76	114	108	94	86	66	160
13	116	127	117	73	96	103	102	94	73	170
14	105	143	112	85	96	96	100	79	82	174
15	106	142	111	99	96	85	82	81	96	177
16	106	135	115	107	110	76	69	92	91	157
17	121	136	89	94	118	102	76	77	79	165
18	104	127	123	108	112	76	67	94	86	153
19	112	138	108	76	105	107	94	94	70	160
20	119	127	111	91	95	101	88	89	77	176
21a	118	110	122	77	114	107	90	86	63	160
21b	111	118	118	108	121	77	61	92	80	146
22	122	125	111	93	91	99	85	96	76	173
23	119	118	116	97	102	99	80	81	82	177
24	121	139	100	96	87	91	80	94	95	175
25	115	129	115	72	104	97	97	104	72	152
26	117	113	109	96	108	76	91	96	76	148
27	105	144	101	118	100	81	80	94	73	153
28	107	150	104	90	104	84	82	102	90	154
29	94	152	114	80	98	98	91	105	80	156
30	106	147	102	106	101	88	86	98	71	154
31	107	153	100	86	107	88	88	100	85	153
32	105	143	112	73	98	101	74	102	97	145
33	110	137	111	82	110	94	79	104	81	145

Table A2. Dihedral angles/$^{\circ}$ found in the zinc complexes.

No.	δ_{45}	δ_{25}	δ_{14}	δ_{12}	δ_{35}	δ_{13}	δ_{23}	δ_{34}	δ_{24}
1	109	112	103	107	91	98	56	57	39
2	106	112	98	103	89	77	50	65	38
3	102	100	111	107	99	73	53	46	45
4	107	109	106	108	89	90	53	82	25
5	103	101	111	111	91	99	58	57	39
6	102	108	103	106	100	99	51	58	43
7	99	99	108	108	99	72	50	50	50
8	115	112	106	118	89	86	58	64	19
9	113	114	121	107	89	90	69	61	13
10	100	108	107	104	98	98	56	55	41
11	105	107	103	104	97	99	52	58	45
12	119	106	114	119	85	88	64	58	15
13	116	103	104	115	98	98	53	52	36
14	111	99	111	110	90	97	66	55	43
15	104	108	114	106	92	95	62	60	42
16	111	114	121	109	89	89	65	60	15
17	101	120	109	127	89	88	49	72	21
18	114	111	121	103	88	84	69	54	17
19	116	111	108	119	90	89	61	65	17
20	105	103	102	110	93	100	54	59	43
21a	113	97	104	111	109	105	54	47	35
21b	111	114	118	106	84	82	63	57	14
22	104	107	99	108	91	78	57	60	42
23	100	102	105	108	80	76	49	54	49
24	103	120	103	114	92	96	46	64	37
25	119	111	111	119	88	88	59	59	14
26	109	111	109	112	87	86	78	56	18
27	115	117	121	114	69	89	82	56	13
28	117	117	115	118	79	79	74	76	5
29	119	115	125	115	81	76	76	71	4
30	119	116	117	113	73	88	80	66	8
31	119	122	116	119	75	78	75	78	0
32	113	114	110	113	84	86	56	85	14
33	110	111	110	113	82	87	73	81	8

Table A3. Interatomic angles/^{o} found in the nickel complexes.

No.	θ_{23}	θ_{24}	θ_{34}	θ_{12}	θ_{13}	θ_{14}	θ_{52}	θ_{53}	θ_{54}	θ_{15}
1	121	127	109	86	101	103	90	85	76	174
2	106	159	95	94	96	87	84	92	92	172
3	102	172	86	81	102	98	98	85	82	173
4	103	170	87	97	85	82	82	102	97	173
5	121	158	80	90	102	91	83	94	89	164
6	82	150	126	93	97	94	87	89	83	174
7	82	155	122	92	98	91	90	93	83	169
8	101	170	89	93	93	86	93	94	86	170
9	97	166	97	99	96	80	80	96	99	168
10	101	157	101	94	95	93	77	95	93	167
11	98	158	102	92	99	95	95	100	72	159
12	112	140	108	86	101	87	87	98	88	161
13	112	144	104	90	88	95	89	99	83	173
14	82	157	121	90	100	89	92	98	82	162
15	97	161	102	90	100	87	86	98	91	162
16	100	159	101	88	101	86	89	99	90	160
17	102	164	94	81	95	98	95	99	81	167
18	82	146	131	97	100	86	89	93	82	166
19	101	149	110	83	100	93	92	99	83	161
20	119	121	114	100	101	95	82	82	81	176
21	120	121	116	96	98	93	84	85	84	176
22	97	159	104	87	99	89	90	101	86	160
23	76	170	114	88	86	92	97	95	92	175
24	95	165	100	82	97	97	96	97	82	166
25	102	152	106	87	96	87	89	100	88	163
26	86	163	105	85	83	84	97	99	94	177
27	101	150	107	92	97	95	86	88	85	175
28	126	131	102	85	96	95	80	94	93	165
29	101	154	105	90	90	93	87	95	88	174
30	85	171	105	84	91	92	91	94	92	173
31	100	154	105	93	91	89	89	105	82	163
32	89	174	95	87	107	95	89	77	88	175
33	118	119	119	96	96	96	84	84	84	180
34	93	168	97	91	104	93	88	81	87	175
35	116	117	117	102	101	100	79	79	79	179
36	114	153	91	100	92	89	71	107	93	157
37	93	163	103	100	92	86	85	100	86	167
38	97	160	102	87	101	92	86	96	91	162
39	98	158	104	87	100	92	92	99	82	161

Table A3. (continued)

No.	θ_{23}	θ_{24}	θ_{34}	θ_{12}	θ_{13}	θ_{14}	θ_{52}	θ_{53}	θ_{54}	θ_{15}
40	99	158	100	94	100	95	83	99	83	161
41	104	153	103	90	102	83	83	102	93	155
42	99	169	92	100	97	78	77	93	103	170
43	96	162	102	84	102	94	91	96	84	162
44	120	120	118	94	95	95	85	87	84	178
45	107	133	120	95	84	91	84	94	92	176
46	119	122	118	90	93	89	88	91	90	176
47	120	120	117	96	96	96	83	84	84	179
48	120	116	124	85	98	89	86	94	87	167
49	99	149	112	94	83	91	94	81	91	164
50	111	127	122	84	93	93	84	93	92	167
51	112	123	124	87	90	92	85	93	92	172
52	122	126	112	90	90	93	88	93	87	177
53	116	133	111	91	89	92	87	94	87	176
54	121	127	112	92	92	91	89	89	88	178
55	117	127	116	89	92	88	90	91	91	177
56	114	127	119	89	94	93	89	88	86	178
57	112	134	114	90	93	87	89	96	87	171
58	120	120	120	90	90	90	90	90	90	180
59	107	141	111	89	92	89	91	94	86	173
60	119	113	127	86	98	86	87	95	87	167
61	112	124	124	90	90	90	90	90	90	180
62	112	125	123	88	91	95	86	91	89	174
63	110	133	116	95	98	89	87	84	88	176
64	111	126	120	95	96	95	85	85	84	179
65	112	122	124	101	109	77	85	85	84	161
66	120	120	120	83	99	91	89	89	88	171
67	117	123	119	89	91	89	91	90	89	178
68	114	122	123	93	101	88	88	85	86	173
69	119	123	117	91	95	92	88	87	87	178
70	121	124	114	91	93	94	86	87	87	178
71	120	122	116	94	95	95	87	85	85	179
72	121	122	117	93	95	91	86	90	85	174
73	103	146	111	93	92	91	88	90	87	177
74	106	141	113	90	92	89	90	91	90	177
75	118	132	110	86	86	96	87	88	96	167
76	113	135	112	87	87	96	87	87	95	169
77	119	125	114	93	95	97	85	85	85	177
78	107	144	109	94	92	87	96	89	83	169

Table A4. Dihedral angles/^{o} found in the nickel complexes.

No.	δ_{45}	δ_{25}	δ_{14}	δ_{12}	δ_{35}	δ_{13}	δ_{23}	δ_{34}	δ_{24}
1	103	105	99	113	96	97	55	61	43
2	113	117	110	117	82	81	69	75	13
3	107	113	114	124	84	77	76	82	1
4	114	125	108	113	77	83	75	81	3
5	109	132	112	103	80	79	57	75	5
6	131	105	131	107	86	88	64	46	19
7	131	108	131	110	81	82	72	54	11
8	114	121	113	120	79	79	79	72	3
9	114	118	118	114	79	79	78	78	2
10	114	119	114	115	76	84	68	75	12
11	123	116	117	116	73	82	82	71	1
12	109	112	110	113	86	88	64	66	15
13	116	118	106	112	81	86	60	64	29
14	132	110	132	112	79	79	77	58	5
15	118	117	120	117	79	77	77	76	0
16	118	117	119	119	79	76	77	76	0
17	113	114	107	115	80	84	78	84	2
18	132	104	133	103	89	90	72	40	19
19	122	115	120	118	79	78	70	65	12
20	99	101	110	111	97	106	52	50	45
21	98	101	110	112	97	108	50	50	44
22	120	116	119	116	78	79	79	75	0
23	130	108	126	102	79	83	76	68	7
24	117	111	115	115	79	81	80	79	0
25	119	117	117	115	79	79	71	70	11
26	121	109	112	101	85	77	84	73	11
27	116	113	116	113	78	78	67	64	27
28	101	118	100	116	96	96	41	72	36
29	117	116	114	114	80	84	65	65	19
30	119	107	118	107	83	80	82	77	3
31	124	118	117	111	72	81	76	71	11
32	112	107	130	126	77	72	75	80	1
33	99	99	106	106	98	95	53	52	52
34	111	110	122	121	75	69	81	80	8
35	99	98	107	105	98	105	54	51	51
36	115	125	112	118	69	88	65	84	6
37	122	118	119	110	73	84	81	71	4
38	121	120	123	122	76	75	71	73	2

Table A4. (continued)

No.	δ_{45}	δ_{25}	δ_{14}	δ_{12}	δ_{35}	δ_{13}	δ_{23}	δ_{34}	δ_{24}
39	127	119	124	120	76	77	70	69	1
40	124	124	121	121	65	75	76	76	1
41	120	123	122	121	75	74	71	74	2
42	111	121	120	119	81	76	74	80	2
43	124	119	124	124	74	72	74	72	0
44	92	92	102	103	91	102	60	61	58
45	107	103	107	97	91	95	63	57	49
46	101	102	102	102	98	98	56	58	50
47	94	96	104	105	94	77	56	58	56
48	101	100	102	102	96	96	59	59	52
49	112	104	113	105	81	81	66	52	50
50	103	104	103	105	93	94	59	62	45
51	103	102	102	102	96	97	59	57	51
52	96	100	94	100	91	93	63	71	56
53	100	103	98	101	94	90	66	71	48
54	99	103	102	106	94	97	56	61	49
55	98	99	98	98	92	90	66	67	54
56	100	96	105	103	93	98	62	59	50
57	103	102	102	101	93	92	73	69	42
58	100	100	107	107	100	107	50	50	50
59	110	106	108	106	93	92	69	63	32
60	102	98	103	99	100	99	60	55	51
61	99	102	98	102	102	102	66	47	47
62	98	98	98	100	95	97	66	60	52
63	101	99	113	109	90	97	63	55	41
64	103	98	107	103	94	98	62	54	50
65	103	97	112	91	98	97	74	47	42
66	99	98	92	95	99	92	64	67	58
67	103	101	103	102	99	98	57	54	51
68	99	93	103	97	96	93	69	59	54
69	99	99	101	102	97	98	58	60	53
70	96	100	100	105	94	99	55	64	54
71	99	99	105	108	97	105	52	53	51
72	96	98	107	99	92	93	58	57	49
73	113	108	113	108	87	90	66	58	31
74	110	106	110	106	92	91	63	59	34
75	96	106	95	106	96	96	51	68	52
76	99	105	99	105	94	95	56	65	49
77	98	100	104	107	94	90	54	61	50
78	105	102	105	105	92	92	78	60	36

Table A5. Dihedral angles(ϕ)/^{o} for nickel compounds.

No.	ϕ
1	53
2	22
3	11
4	12
5	27
6	30
7	26
8	13
9	18
10	24
11	26
12	43
13	36
14	28
15	26
16	28
17	21
18	35
19	36
20	58
21	58
22	29
23	10
24	21
25	32
26	12
27	30
28	49
29	26
30	10
31	29
32	7
33	59
34	12
35	60
36	30
37	19
38	26
39	29
40	27
41	36
42	15
43	26

REFERENCES

1. Pancir, J. *J. Amer. Chem. Soc.* 1982, *104*, 7424.
2. Parr, R. G. "Quantum Theory of Molecular Electronic Structure"; Benjamin: New York, Amsterdam, 1964.
3. Liu, B. *J. Chem. Phys.* 1973, *58*, 1925.
4. Bent, H. A. *Chem. Rev.* 1968, *68*, 587.
5. a) Dunitz, J. D. "X-Ray Analysis and the Structure of Organic Molecules"; Cornell University Press: Ithaca, London, 1979.

   b) Bürgi, H. B. *Angew. Chem., Intern. Ed.* 1975, *14*, 460.

   c) Bürgi, H. B.; Dunitz, J. D. *Acc. Chem. Res.* 1983, *16*, 153.
6. Bürgi, H. B. *Inorg. Chem.* 1973, *12*, 2321.
7. Pauling, L. *J. Amer. Chem. Soc.* 1947, *69*, 542.
8. Britton, D.; Dunitz, J. D. *J. Amer. Chem. Soc.* 1981, *103*, 2971.
9. Bürgi, H. B.; Dunitz, J. D.; Shefter, E. *J. Amer. Chem. Soc.* 1973, *95*, 5065.
10. Bürgi, H. B.; Dunitz, J. D.; Shefter, E. *Acta Cryst.* 1974, *B30*, 1517.
11. Bürgi, H. B.; Lehn, J. M.; Wipff, G. *J. Amer. Chem. Soc.* 1974, *96*, 1956.
12. Murray-Rust, P.; Bürgi, H. B.; Dunitz, J. D. *J. Amer. Chem. Soc.* 1975, *97*, 921.
13. Berry, R. S. *J. Chem. Phys.* 1960, *32*, 933.
14. Muetterties, E. L.; Guggenberger, L. J. *J. Amer. Chem. Soc.* 1974, *96*, 1748.
15. Holmes, R. R. *Acc. Chem. Res.* 1979, *12*, 257.
16. Bürgi, H. B.; Shefter, E.; Dunitz, J. D. *Tetrahedron* 1975, *31*, 3089.
17. Chadwick, D. J.; Whittleton, S. N.; Small, R. W. H. *J. Chem. Soc. Perkin Trans.* II 1982, 669.

18. Hutchings, M. G. *J. Chem. Soc. Perkin Trans.* II 1982, 1241.

19. Bye, E.; Schweizer, W. B.; Dunitz, J. D. *J. Amer. Chem. Soc.* 1982, *104*, 5893.

20. Chandrasekhar, K.; Bürgi, H. B. *J. Amer. Chem. Soc.* 1983, *105*, 7081.

21. Bürgi, H. B.; Hownshell, W. D.; Nachbar, R. B.; Mislow, K. *J. Amer. Chem. Soc.* 1983, *105*, 1427.

22. Mealli, C.; Midollini, S.; Moneti, S.; Sacconi, L.; Silvestre, J.; Albright, T. A. *J. Amer. Chem. Soc.* 1982, *104*, 95.

23. Basolo, F.; Pearson, R. G. "Mechanisms of Inorganic Reactions", 2nd ed.; Wiley: New York, 1967.

24. Anderson, G. K.; Cross, R. J. *Chem. Soc. Rev.* 1980, *9*, 185.

25. Kennard, O.; Watson, D. G.; Allen, F. H.; Motherwell, F.D.S.; Town, W. G.; Rodgers, J. *Chem. Brit.* 1975, *11*, 213.

26. Ito, T. *Acta Cryst.* 1972, *B28*, 1697.

27. Powell, H. M.; Watkin, D. J.; Wilford, J. B. *J. Chem. Soc. (A)* 1971, 1803.

28. Raymond, N. K.; Corfield, P. W. R.; Ibers, J. A. *Inorg. Chem.* 1968, *7*, 1362.

29. Pauling, L. "The Nature of the Chemical Bond"; Cornell University Press: Ithaca, New York, 1960.

30. Ugi, I.; Marquarding, D.; Klusacek, H.; Gillespie, P.; Ramirez, F. *Acc. Chem. Res.* 1971, *4*, 288.

31. Altmann, J. A.; Yates, K.; Csizmadia, I. G. *J. Amer. Chem. Soc.* 1976, *98*, 1450.

32. Russegger, P.; Brickman, J. *Chem. Phys. Lett.* 1975, *30*, 276.

33. Favas, M. C.; Kepert, D. L. *Prog. Inorg. Chem.* 1980, *27*, 325.

34. Wolfe, S.; Mitchell, D. J.; Schlegel, H. B. *J. Amer. Chem. Soc.* 1981, *103*, 7692.

35. Rossi, A. R.; Hoffmann, R. *Inorg. Chem.* 1975, *14*, 365.

36. Burdett, J. K. *Adv. Inorg. Chem. Radiochem.* 1978, *21*, 113.

37. Gillespie, R. J. *J. Chem. Soc.* 1963, 4679.

38. Gillespie, R. J. *J. Chem. Soc.* 1963, 4672.

39. Muetterties, E. L. *MTP Int. Rev. Sci.* 1972, *10*, 46.

40. Bürgi, H. B. *private communication.*

41. Gleizes, A.; Kerkeni, A.; Dartiguenave, M.; Dartiguenave, Y.; Klein, H. F. *Inorg. Chem.* 1981, *20*, 2372.

42. Saint-Joly, C.; Mari, A.; Gleizes, A.; Dartiguenave, M.; Dartiguenave, Y.; Galy, J. *Inorg. Chem.* 1980, *19*, 2403.

43. Meier, P. F.; Merbach, A. E.; Dartiguenave, M.; Dartiguenave, Y. *Inorg. Chem.* 1979, *18*, 610.

44. Lukosius, E. J.; Coskran, K. J. *Inorg. Chem.* 1975, *14*, 1926.

45. Pellerite, M. J.; Brauman, J. I. *J. Amer. Chem. Soc.* 1983, *105*, 2672.

46. Kita, H.; Tanaka, K.; Tanaka, T. *Inorg. Chim. Acta* 1977, *21*, 229.

47. Raston, C. L.; White, A. H.; Winter, G. *Aust. J. Chem.* 1976, *29*, 731.

48. Eaton, D. R.; Zaw, K. *J. Inorg. Nucl. Chem.* 1976, *38*, 1007.

49. Fackler, J. P.; Fetchin, J. A. *J. Amer. Chem. Soc.* 1970, *92*, 2912.

50. Mirti, P.; Gennaro, M. C.; Vallinotto, M. *Trans. Met. Chem.* 1982, *7*, 2.

51. Fackler, J. P.; Fetchin, J. A.; Fries, D. C. *J. Amer. Chem. Soc.* 1972, *94*, 7323.

52. Gupta, R. K.; Pesando, J. M. *J. Biol. Chem.* 1975, *250*, 2630.

53. Kannan, K. K.; Pelef, M.; Fridborg, K.; Cid-Dresner, M.; Löugren, S. *F.E.B.S. Letters* 1977, *73*, 115.

54. Dworschach, R. T.; Plapp, B. V. *Biochemistry* 1977, *16*, 2716.

55. Argos, P.; Garavito, R. M.; Eventoff, W.; Rossman, M. G.; Branden, C. I. *J. Mol. Biol.* 1978, *126*, 141.

56. Alcock, N. W.; Herron, N.; Moore, P. *J. Chem. Soc. Dalton Trans.* 1978, 1282.

57. Hynes, M. J.; Brannick, P. F. *J. Chem. Soc. Dalton Trans.* 1977, 2281.

58. Cusumano, M.; Ricevuto, V.; Romeo, R.; Trozzi, M. *Atti. Accad. Peloritana Pericolanti, Cl. Sci. Fis., Mat. Nat.* 1974, *54*, 157. (*Chem. Abs.* 1976, 85:37574.)

59. Schumann, M.; Holtum, A. v.; Wannowius, K. J.; Elias, H. *Inorg. Chem.* 1982, *21*, 606.

60. Fayyaz, M. U.; Grant, M. W. *Aust. J. Chem.* 1978, *31*, 1439.

61. English, A. D.; Meakin, P.; Jesson, J. P. *J. Amer. Chem. Soc.* 1976, *98*, 422.

62. Wada, M.; Nishiwaki, K. *J. Chem. Soc. Dalton Trans.* 1983, 1841.

63. Funke, L. A.; Melson, G. A. *Inorg. Chem.* 1975, *14*, 306.

64. Sarkar, B. *Coord. Chem.* 21, "Proc. of the 21st I.C.C.C.", Toulouse, France, 7-11 July 1980; Pergamon Press, 1980.

65. Meakin, P.; Jesson, J. P. *J. Amer. Chem. Soc.* 1974, *96*, 5751.

66. Garrou, P. E.; Heck, R. F. *J. Amer. Chem. Soc.* 1976, *98*, 4115.

67. Dartiguenave, M.; Dartiguenave, Y.; Gleizes, A.; Saint-Joly, C.; Galy, J.; Meier, P.; Mehrbach, A. E. *Inorg. Chem.* 1978, *17*, 3503.

68. Grimes, C. G.; Pearson, R. G. *Inorg. Chem.* 1974, *13*, 970.

69. Lukosius, E. J.; Coskran, K. J. *Inorg. Chem.* 1975, *14*, 1922.

70. Sweigart, D. A. *Inorg. Chim. Acta* 1977, *23*, L13.

71. Cusumano, M. *J. Chem. Soc. Dalton Trans.* 1976, 2133.

72. Dapporto, P.; Morassi, R.; Sacconi, L. *J. Chem. Soc.* (A) 1970, 1298.